

Review

Open Access



Two-dimensional materials: synthesis and applications in the electro-reduction of carbon dioxide

Yaoyu Yin^{1,2}, Xinchen Kang^{1,2,*} , Buxing Han^{1,2,3,*}

¹Beijing National Laboratory for Molecular Sciences, Key Laboratory of Colloid and Interface and Thermodynamics, Institute of Chemistry, Chinese Academy of Sciences, Beijing 100190, China.

²School of Chemistry, University of Chinese Academy of Sciences, Beijing 100049, China.

³Shanghai Key Laboratory of Green Chemistry and Chemical Processes, School of Chemistry and Molecular Engineering, East China Normal University, Shanghai 200062, China.

***Correspondence to:** Prof. Xinchen Kang, Beijing National Laboratory for Molecular Sciences, Key Laboratory of Colloid and Interface and Thermodynamics, Institute of Chemistry, Chinese Academy of Sciences, Beijing 100190, China. E-mail: kangxinchen@iccas.ac.cn; Prof. Buxing Han, Beijing National Laboratory for Molecular Sciences, Key Laboratory of Colloid and Interface and Thermodynamics, Institute of Chemistry, Chinese Academy of Sciences, Beijing 100190, China. E-mail: hanbx@iccas.ac.cn

How to cite this article: Yin Y, Kang X, Han B. Two-dimensional materials: synthesis and applications in the electro-reduction of carbon dioxide. *Chem Synth* 2022;2:19. <https://dx.doi.org/10.20517/cs.2022.20>

Received: 28 Aug 2022 **First Decision:** 22 Sep 2022 **Revised:** 5 Oct 2022 **Accepted:** 9 Nov 2022 **Published:** 28 Nov 2022

Academic Editors: Bao-Lian Su, Da-Gang Yu **Copy Editor:** Peng-Juan Wen **Production Editor:** Peng-Juan Wen

Abstract

The emission of CO₂ has become an increasingly prominent issue. Electrochemical reduction of CO₂ to value-added chemicals provides a promising strategy to mitigate energy shortage and achieve carbon neutrality. Two-dimensional (2D) materials are highly attractive for the fabrication of catalysts owing to their special electronic and geometric properties as well as a multitude of edge active sites. Various 2D materials have been proposed for synthesis and use in the conversion of CO₂ to versatile carbonous products. This review presents the latest progress on various 2D materials with a focus on their synthesis and applications in the electrochemical reduction of CO₂. Initially, the advantages of 2D materials for CO₂ electro-reduction are briefly discussed. Subsequently, common methods for the synthesis of 2D materials and the role of these materials in the electrochemical reduction of CO₂ are elaborated. Finally, some perspectives for future investigations of 2D materials for CO₂ electro-reduction are proposed.



© The Author(s) 2022. **Open Access** This article is licensed under a Creative Commons Attribution 4.0 International License (<https://creativecommons.org/licenses/by/4.0/>), which permits unrestricted use, sharing, adaptation, distribution and reproduction in any medium or format, for any purpose, even commercially, as long as you give appropriate credit to the original author(s) and the source, provide a link to the Creative Commons license, and indicate if changes were made.



Keywords: 2D materials, material synthesis, electrochemical reduction of CO₂

INTRODUCTION

The concentration of greenhouse gas CO₂ has risen by 100 ppm since the industrial revolution. The average temperature has been rising at an average rate of 0.1 °C per decade for nearly half a century, which results in serious global warming^[1-3]. From another perspective, CO₂ is an abundant, clean, and cheap feedstock for the production of value-added chemicals. Hence, it is of great ecological and social significance to utilize and convert CO₂ into high-value-added chemical products^[4-6]. Nonetheless, CO₂ has thermodynamically stable and chemically inert properties, and thus its conversion is highly energy intensive. Considering the prominent role of CO₂ in global warming and the chemical characteristics of CO₂, numerous chemical technologies have been developed for CO₂ conversion, including thermal catalysis^[7-9], photocatalysis^[10-12], and electrocatalysis^[13-15]. The development of highly effective catalysts and related equipment for CO₂ transformation has boomed in recent years^[16]. Among them, the electro-reduction of CO₂ to value-added chemicals benefits from low investment in equipment, high efficiency, and environmental acceptance^[17-20].

The electrochemical reduction of CO₂ is a multi-electron transfer process, which mainly occurs at the electrode and the electrolyte interface. This process consists of four steps: (i) CO₂ is chemically adsorbed on the electrode surface; (ii) CO₂ is converted into CO₂^{•-} by one-electron attacks; (iii) Multiple electrons and protons are transferred to CO₂^{•-} for the construction of C-H and C-C bonds; and (iv) Products are released from the electrode^[21]. The half-reactions and corresponding standard reduction potentials for the electro-reduction of CO₂ to various products have been elucidated through thermodynamic studies, as illustrated in [Figure 1](#).

The electro-reduction of CO₂ to related products is a multi-step reduction. In spite of the low chemical reactivity of CO₂, the theoretical potential required for products is not a large negative value^[22]. In fact, the first hurdle of CO₂ electro-reduction is the potential barrier for CO₂ activation (CO₂ + e⁻ = CO₂^{•-}), which is -1.90 V *vs.* the standard hydrogen electrode (SHE). Because different products require similar thermodynamic potentials, it is challenging to obtain the desired product with high selectivity^[23,24]. Accordingly, the development of electrode materials is significant to realize efficient electro-reduction with high selectivity toward target products.

Current density and selectivity are two evaluation indicators in CO₂ electro-reduction. A large current density indicates a fast reaction rate to provide a high yield of products from CO₂, and high selectivity can ease separation to reduce cost. Electrode materials play a decisive role in electrocatalytic performance. Hence, the design and synthesis of electrode materials with high activity, selectivity, and stability are significant for highly efficient CO₂ electro-reduction. 2D materials are defined as a type of nanomaterials with a layer-like morphology and small thickness (normally 1-100 nm) in which electrons move on the nanoscale in two dimensions^[25]. 2D materials have been developed for various applications, such as energy conversion^[26-28], catalysis^[29-31], sensing^[32-34], photodetector^[35-37], and memristor^[38-40], owing to their unique 2D geometry, nanoscale thickness, and high surface-to-volume ratio. 2D structures, such as nanoplates, nanosheets, and nanoflakes, have been used for preparation of various materials, including metals, metal oxides, metallic sulfides, and carbon materials^[41-44]. Until now, numerous 2D materials have been designed and prepared for CO₂ electro-reduction^[45-47]. For commercial applications of electrocatalysts, high yield and controllable fabrication techniques are essential. Versatile methods for the preparation of 2D materials, such as exfoliation, extraction, chemical or physical vapor deposition, and wet-chemical synthesis, have been developed. Different synthesis routes have different advantages. These strategies determine the morphology

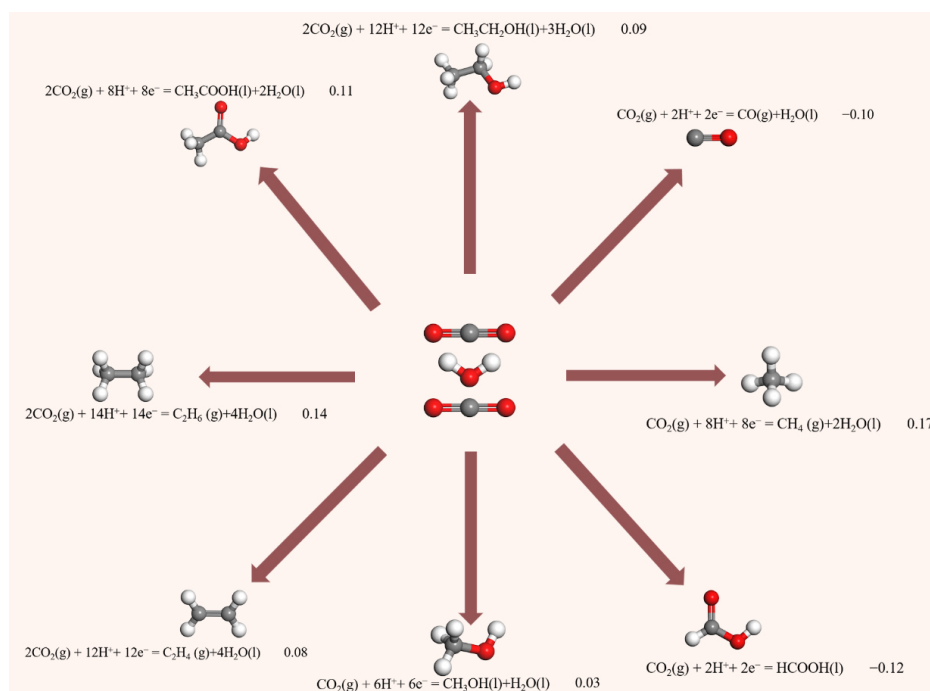


Figure 1. Half reactions and corresponding standard reduction potentials vs. reversible hydrogen electrode (RHE) (E⁰/V vs. RHE) for the electrochemical reduction of CO₂ to various products.

of materials and further affect their properties, providing opportunities for their utilization in electrocatalysis.

This review covers the current progress on CO₂ electro-reduction using 2D material electrodes with a focus on the (i) advantages of 2D materials for CO₂ electro-reduction, (ii) strategies for 2D nanomaterial synthesis, and (iii) catalytic performance of 2D materials in the electrochemical reduction of CO₂.

ADVANTAGES OF 2D NANOSTRUCTURES FOR CO₂ ELECTRO-REDUCTION

Electrochemical reduction of CO₂ is a process involving gas-solid-liquid interactions^[48,49], and its current density and Faradaic efficiency (FE) are largely affected by the specific surface area of electrode materials. Generally, a higher specific surface area guarantees more adsorption and active sites, leading to better catalytic performance. In addition, the concentration gradient of CO₂ and reaction intermediates are related to CO₂ diffusion on the electrode surface. The adsorption/desorption thermodynamics and kinetics of intermediates determine the selectivity and production rate of target products. Thus, materials with special morphologies and structures play a crucial role in catalyzing this process.

The electrochemical reduction of CO₂ is surface reaction, and thus 2D materials are suitable as catalysts because of the following advantages. First, 2D materials have a unique planar structure, which promotes interactions with the substrate or active components as well as the formation of heterojunctions to realize comprehensive regulation of electrocatalysis^[50]. Second, 2D materials have enhanced electronic properties, such as high electron mobility and carrier concentration^[51,52], which increase electron transfer from the electrode to CO₂. Third, 2D materials have a high proportion of uncoordinated sites and large specific surface areas, which increases interactions between CO₂ and the catalyst^[53]. Exposed surface atoms in 2D materials can escape from their respective lattices to form defect sites, and these thermodynamically

unstable sites can trap electrons and shorten electron transport and ion diffusion distances^[54,55]. Owing to the low atomic coordination number at the edge, the activity at the edge is higher than that at the basal plane in 2D materials^[56]. Fourth, a multi-layer or single-layer structure increases the confinement effect, which improves the catalytic performance^[57,58]. The surface of 2D materials can be modified to produce special gas trapping cavities, where interactions between the electrode, electrolyte, and CO₂ gas are enhanced^[59,60]. Fifth, pores in 2D materials are fully exploited owing to the ultrathin structure. Porous structures in 2D materials can effectively amplify the differences in mass transfer efficiency as well as intermediate diffusion during CO₂ reduction.

In summary, 2D materials have geometries, electronic structures, and defects that are suitable for CO₂ electro-reduction. Owing to their large specific surface area, 2D materials can serve as supports for hybrid materials. In addition, the unique atomic-layer-thick structure provides an ideal platform for revealing atomic-scale mechanisms. The rational development and exploitation of distinct structural and electronic properties of 2D materials endow 2D materials with more opportunities for broad applications in the field of CO₂ electro-reduction.

SYNTHESIS OF 2D NANOSTRUCTURES

The electrocatalytic performances of 2D materials are mainly determined by the morphology, structure and chemical properties of the materials, which in turn are closely related to the synthesis methods. Since the discovery of graphene, many efficient routes have been developed for the synthesis of 2D materials, allowing researchers to design more promising 2D materials. Top-down and bottom-up routes are commonly used for the synthesis of 2D materials^[61-63]. Top-down routes, such as exfoliation and extraction procedures, are easily performed without special equipment, and thus they are effective for the synthesis of inorganic materials, such as graphene and metal dichalcogenides. Bottom-up routes, including chemical/physical vapor deposition and wet-chemical syntheses, provide 2D materials with accurately controlled morphologies and structures, and thus they are frequently used to prepare materials with unique structures. In this section, several typical routes for the fabrication of 2D materials are briefly described.

Exfoliation

Exfoliation requires external mechanical forces to peel off 2D materials with a single or few layers from bulk objects. This method relies on driving forces, such as mechanical and ultrasonic forces, to overcome intermolecular interactions, such as the van der Waals force, between atomic layers. This process is simple to operate and produces few defects in the resulting material, although it suffers from low effectiveness and poor repeatability, which limits its practical applications.

Mechanical exfoliation has been a common method for the fabrication of emergent 2D materials [Figure 2A] since Geim obtained graphene by tearing off graphite from tape^[64]. Other research groups have since developed similar methods for producing high-quality 2D materials. Li *et al.* used bulk materials to isolate desired products and prepare various single- and few-layer transition-metal dichalcogenide nanosheets with high crystallinity, including WSe₂, TaS₂, and TaSe₂^[65]. However, the yield is low and the thickness and size of as-prepared materials are difficult to control using this strategy, thus inhibiting large-scale production. Huang *et al.* used a universal, one-step method via Au-assisted mechanical exfoliation to address the above problem [Figure 2B] and synthesize a series of 2D materials such as BP, RuCl₃, Fe₃GeTe₂, FeSe, MoS₂, and WSe₂^[66] [Figure 2C]. This environmentally compliant route meets the requirements of green chemistry. Field-effect transistor devices have been fabricated using 2D MoS₂ and WSe₂. However, the use of noble metals undoubtedly increases the cost, thus hampering the implementation of this route for the fabrication of large devices.

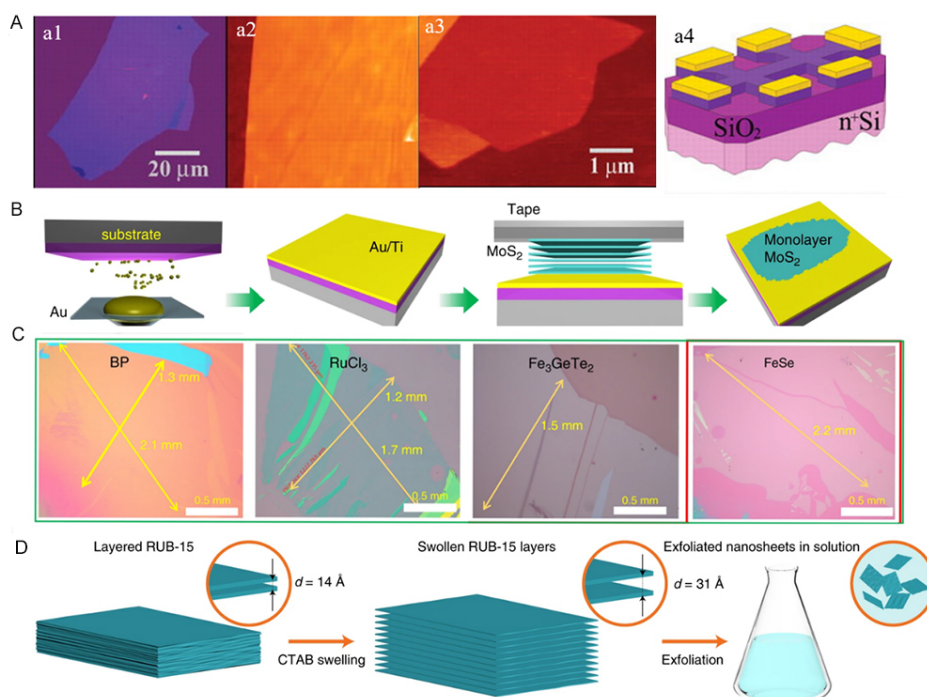


Figure 2. Synthesis of 2D materials by exfoliation. (A) Graphene films synthesized by mechanical exfoliation^[64]. (B) Schematic diagram of Au-assisted mechanical exfoliation^[66]. (C) 2D materials synthesized by Au-assisted mechanical exfoliation^[66]. (D) Schematic diagram of CTAB-assisted material swelling^[69]. 2D: 2-dimensional; CTAB: hexadecyl trimethyl ammonium bromide.

Ultrasonic exfoliation in the liquid phase relies on the cavitation effect. When bulk materials are subjected to an ultrasonic wave in a suitable solvent, micro-gas core cavitation bubbles produced in the solvent expand the space between the layers of the material, thus producing the 2D material. Coleman *et al.* reported in detail that ultrasonic exfoliation of transition metal dichalcogenides, such as BN, MoS₂, WS₂, MoSe₂, MoTe₂, TaSe₂, NbSe₂, NiTe₂, and Bi₂Te₂, in organic solvents can be used to produce 2D materials with few layers^[67]. Metal oxide and hydroxide with limited layers can also be produced by ultrasonic exfoliation. Compared with transition metal dichalcogenides, which are stabilized by weak intermolecular interactions, such as the van der Waals force, metal oxides and hydroxides are stabilized by strong ionic interactions, which makes exfoliation difficult^[68]. Although ultrasonic exfoliation is the most promising strategy for the industrial production of 2D materials, this strategy has fatal defects. For example, (i) the number of layers and thickness are difficult to control and (ii) the recovery rate is low, which confines the method to the laboratory.

Intercalation-based exfoliation has been widely explored owing to the unique characteristics of high-yield monolayers. Suitable intercalation species are vital for effective intercalation and determine whether intercalation proceeds. For example, surfactants are often used for the production of 2D nanosheets. Dakhchoune *et al.* reported that intercalation of surfactant hexadecyl trimethyl ammonium bromide (CTAB) into sodalite precursors leads to material swelling^[69]. Consequently, the lattice spacing increases from 1.4 nm to 3.1 nm [Figure 2D], indicating that interlayer interactions are weakened by the intercalation of CTAB.

Chemical vapor deposition

Chemical vapor deposition (CVD) is one of the most commonly used methods for the synthesis of 2D materials^[70]. In this technique, a thin solid layer is deposited on the surface of a substrate through vapor-

phase chemical reactions in a high-temperature gas. Various solid-state layers (e.g., single crystals, continuous thin films, and heterojunctions) can be produced on substrates by adjusting the operating temperature, flow gas species, phase composition, and substrate. Numerous functional van der Waals heterostructures can also be created by this method^[71] [Figure 3A-D]. In contrast to exfoliation and extraction, CVD allows control of the number of layers as well as the density and purity of products through changes in the synthesis conditions.

CVD has become an important method for the preparation of 2D materials since it was used to prepare graphene in 2009^[72,73]. Browne *et al.* synthesized MoS₂ and WS₂ materials to serve as electrodes^[74]. The surface of as-prepared MoS₂/WS₂ is rougher than that of commercial materials. Li *et al.* used methane to prepare graphene films with a large surface area on a copper substrate by CVD^[73]. The as-prepared graphene film can be easily transferred to alternative substrates for the fabrication of functional devices. Yin *et al.* synthesized high-quality nonlayered Fe₂O₃ nanosheets with a thickness of 1.95 nm, which exhibit lattice relaxation owing to the ultrathin structure^[75]. Although the growth of 2D materials on substrates is rapid, the direct growth of 2D metal/metal oxides onto substrates is restricted because of the high melting point of metals/metal oxides. Introducing molten salts as additives can effectively reduce the reaction temperature and promote the growth of high-quality 2D materials. For instance, Zhou *et al.* reported a new method to synthesize 47 compounds by adding NaCl and KI as adjuvants^[76]. Despite various efforts focused on synthesizing 2D materials by CVD, poor repeatability and unscalable production restrict the industrial application of CVD.

As mentioned above, the thickness and size of 2D materials can be precisely controlled by adjusting the working temperature, carrier gas rate, and chamber pressure. Space-confined CVD can be used to achieve the growth of high-quality 2D materials. Recently, Li *et al.* used Te-assisted CVD to precisely synthesize 2D Fe single-crystal nanoflakes with different thicknesses^[77] [Figure 3E-G]. Xu *et al.* used space-confined CVD to grow homogeneous 1T'-MoTe₂ monolayers with a lateral size of 100 μm in batches, demonstrating that the confined space can increase the vapor pressure of sulfur to extend the lifetime of monolayer tellurides from several minutes to at least 24 h^[78].

Hydrothermal and solvothermal methods

Hydrothermal and solvothermal methods are widely used to prepare various 2D materials with high yields. Both methods are based on heterogeneous chemical reactions occurring at high temperature and pressure during which substances are dissolved and recrystallized. The difference between the two methods is the solvent. Water is used as the solvent in hydrothermal methods, while non-aqueous organic solvents are used in solvothermal methods. Materials prepared by hydro/solvothermal methods have advantageous characteristics, such as high crystallinity, small particle size, and uniform distribution.

Among various 2D materials, metal oxides have attracted considerable attention in the fields of catalysis, energy conversion, and electronics owing to their low cost and large surface area. Sun *et al.* developed a general solvothermal method to prepare various transition metal oxide nanosheets, such as ZnO, WO₃, Co₃O₄ and TiO₂, [Figure 4] in different solvents (water/ethanol/glycol) for use in photoelectric or photochemical devices^[79]. The thickness of as-prepared nanosheets ranges from 1.6 nm to 5.2 nm. Metal-organic frameworks (MOFs) represent a class of hybrid materials comprising ordered networks formed by combining metal ions with organic ligands^[80-82]. MOFs have been explored extensively to prepare 2D structures. As a bottom-up synthesis method, the templated hydrothermal strategy induces the confined growth of 2D MOF materials. Zheng *et al.* synthesized ultrathin 2D Co-MOF with a thickness of 2 nm by reacting precursors and polyvinyl pyrrolidone in DMF/C₂H₅OH solution at 80 °C for 80 h^[83]. Moreover,

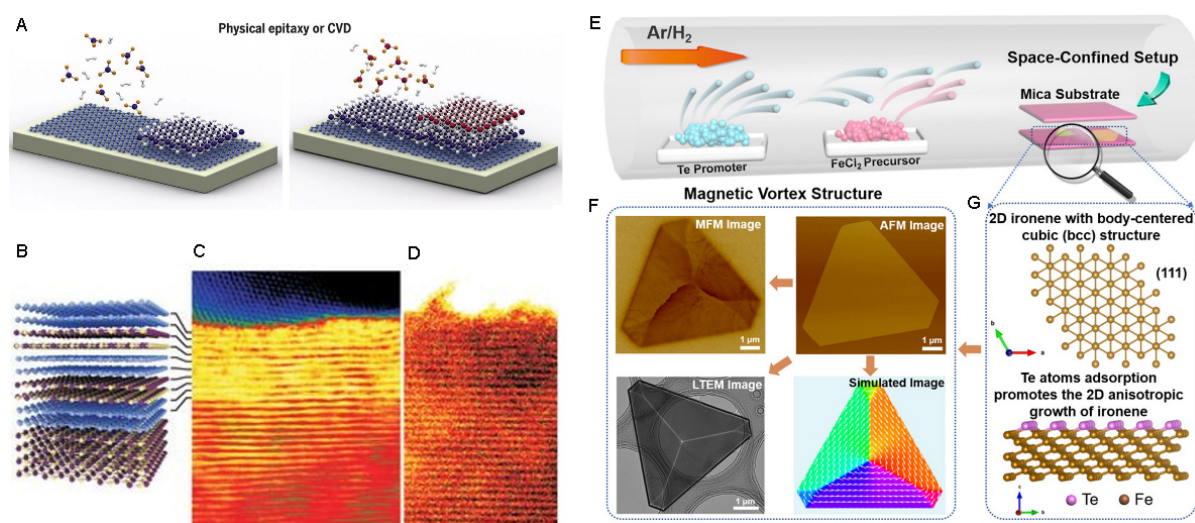


Figure 3. Synthesis of 2D materials by CVD. (A) Schematic diagram of the CVD method. (B-D) Schematic diagram and TEM images of graphene/hBN heterostructures. Here, carbon atoms are represented by blue spheres, boron is shown in yellow, and nitrogen is in purple^[71]. (E-G) Synthesis of 2D Fe single-crystal nanoflakes by space-confined CVD^[77]. 2D: 2-dimensional; CVD: chemical vapor deposition; TEM: transmission electron microscopy.

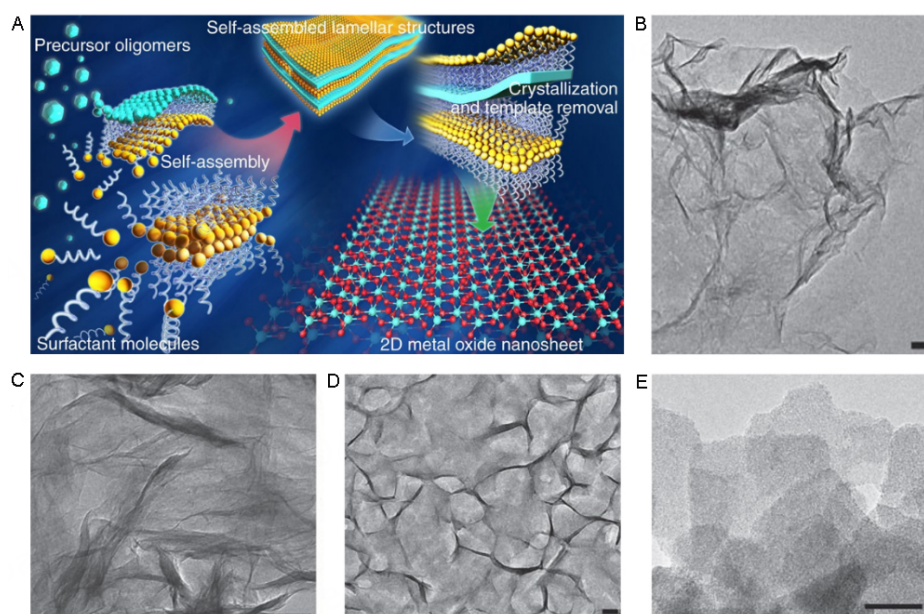


Figure 4. Synthesis of 2D metal oxide nanosheets by the hydrothermal method. (A) Schematic diagram of the synthesis route. TEM images of (B) Co_3O_4 , (C) TiO_2 , (D) ZnO , and (E) WO_3 ^[79]. 2D: 2-dimensional; TEM: transmission electron microscopy.

various novel 2D materials, such as MoP@In-PC , Mo-Bi bimetallic, $\text{Sn}_4\text{P}_3/\text{rGO}$, have been synthesized by hydro/solvothermal methods^[84-86].

Electrodeposition

Electrochemical deposition is a liquid-phase process based on redox reactions by which 2D materials are easily formed. This method has numerous advantages, including mild conditions, low cost, high safety, easy operation, and high controllability. The morphology, structure, and physicochemical property of products

can be controlled by adjusting various conditions, including the pH of the solution, potential, time, and temperature, during electrodeposition.

Electrodes prepared by electrodeposition have very low contact resistance, which promotes electron transfer in functional devices. Rabiee *et al.* grew uniform Bi-based nanosheets on a substrate by pulse electrodeposition^[87]. In contrast, a Bi-based bulk material was obtained by continuous electrodeposition. Abdelazim *et al.* reported the lateral growth of MoS₂ on an insulating surface^[88]. The highly anisotropic growth rate of MoS₂ can be controlled by simple electrodeposition to obtain a lateral to vertical growth ratio exceeding 20. This paves a new pathway to precisely control the growth direction to obtain 2D materials. Polymetallic alloys have shown great potential in various applications, and co-deposition of versatile metals can be realized with electrodeposition by adjusting the pH of the solution or applied voltage. For example, Feng *et al.* used electrodeposition in a solution of pH 10 to obtain an active borate-intercalated NiCoFe-LDH, which is susceptible to redeposition to recover catalytic activity, further confirming the advantage of electrodeposition^[89]. Shen *et al.* synthesized amorphous 2D FeMn by electrodeposition using sodium citrate as a structure-directing agent^[90] [Figure 5A-C]. OH⁻ is produced near the surface of the cathode, and metal ions are deposited with OH⁻ at the cathode to form hydroxides.

Despite recent achievements in the electrodeposition of 2D materials, the mechanism remains difficult to demonstrate. Tan *et al.* used transmission electron microscopy (TEM) to visualize material synthesis, including nucleation sites, growth mechanisms, and structures formed during electrochemical reactions^[91]. This promising technology can be used to observe an electron beam-stable and low-contrast extended electrode area with high resolution [Figure 5D].

Extraction

To date, many new types of 2D materials have been developed for functional devices. 2D transition metal carbides and nitrides (MXenes) have good electrical properties owing to the inner conductive carbide layer and hydrophilic transition metal oxide surface, and thus they are promising materials for the fabrication of batteries and catalysts.

The most effective synthesis route of MXenes is the selective etching of “A” layers from an Al-containing MAX phase, where A represents a III A or IV A element (e.g., Al, Ga, Si, or Ge) and X represents either C or N. Lukatskaya *et al.* and Ghidui *et al.* synthesized various MXenes by selective extraction, electrochemical etching, and ion intercalation^[92-94]. The as-prepared 2D materials are applied in Li-ion batteries, which acquire excellent electricity performance.

In addition to the methods above, researchers have explored many other routes for the synthesis of 2D materials. Among the multitude of strategies, templated synthesis can easily and directly realize 2D materials with controlled structures. For example, Liu *et al.* synthesized a series of mesoporous materials with a single-layer structure^[95]. Phenolic formaldehyde resin, a flexible template, is beneficial for the adsorption and subsequent confinement of inorganic precursors on the salt surface. Surface-limited cooperative assembly allows for large-scale production, and 14.1 g of mesoporous TiO₂ with single-layer structure can be synthesized per batch. Although templated synthesis has been extensively explored for the preparation of 2D materials, the long preparation time and high cost restrict its wide application in industry. Developing template-free preparation methods is of significance for the mass production of 2D materials. Zhang *et al.* developed a general method for control-oriented growth of MOF nanosheets with ultrathin thicknesses and abundant unsaturated coordination metal sites using CO₂ as a capping agent^[96]. The process is template-free and CO₂ can be easily removed by depressurization after synthesis. Atomic

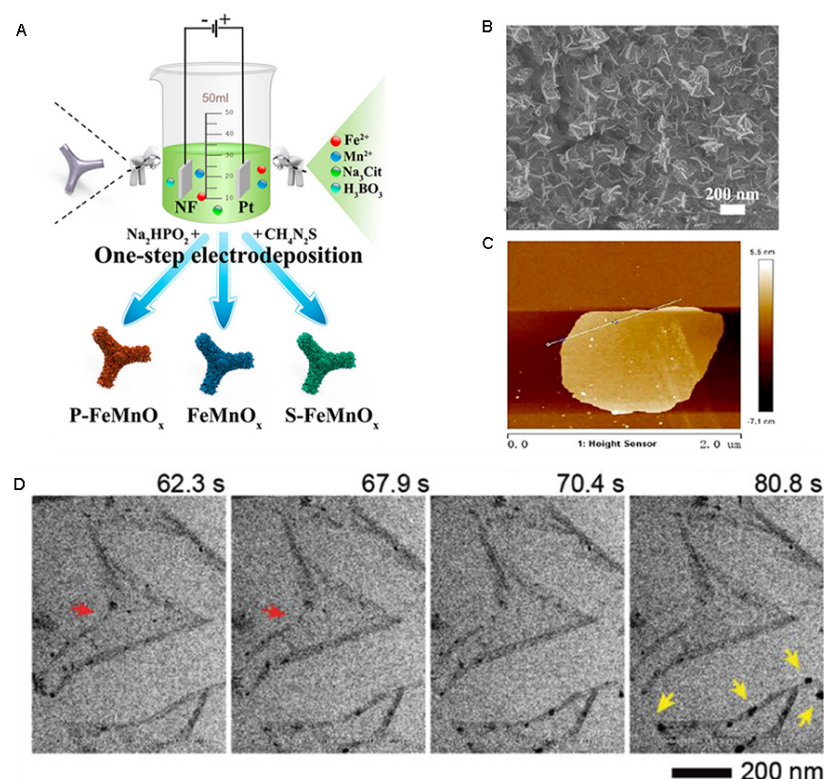


Figure 5. Synthesis of 2D materials by electrodeposition. (A) Schematic diagram of the preparation of FeMn-based nanosheets. (B) SEM image of FeMnO_x . (C) AFM image of FeMnO_x ^[90]. (D) TEM image of MoS_2 flake after exposure to the electron beam^[91]. 2D: 2-dimensional; TEM: transmission electron microscopy.

layer deposition has emerged as a powerful technique to prepare nanofilms with a thickness approaching the Debye length. Ko *et al.* reported the preparation of a large-area WS_2 nanosheet with a precisely controlled number of layers by atomic layer deposition^[97]. These methods can be used for reference and guidance in the development and application of 2D materials for CO_2 electrocatalytic reduction.

ELECTROCHEMICAL REDUCTION OF CO_2 OVER 2D NANOSTRUCTURES

Various 2D nanostructures have been extensively explored for the electro-reduction of CO_2 owing to their unique structure and properties. Versatile electrode materials, including metals, metal oxides, metal dichalcogenides, and carbon-based nanomaterials, have shown potential in CO_2 electrocatalytic reduction [Table 1]. In this section, advances in 2D materials for CO_2 electrocatalytic reduction are reviewed and the related mechanism is discussed.

Metal materials

Zero-valence metals are the most popular electrode materials for CO_2 electro-reduction owing to their high conductivity, high stability, controllable crystal faces, and ease of CO_2 activation.

Noble metals

Noble metals are considered the most effective catalysts^[114,115], and electrochemical reduction of CO_2 over noble metal-based electrodes has been extensively studied in recent years^[116,117]. The particle size determines the catalytic performance because larger particles have fewer active sites, whereas smaller particles favor H_2 evolution over CO_2 reduction. Noble metal nanosheets exhibit excellent catalytic performance in CO_2

Table 1. Summary of 2D-based materials developed for CO₂ electrocatalytic reduction

Catalysts	Electrolyte	Products	FE	Potential	<i>j</i> (mA cm ⁻²)	Refs.
Ag nanosheet	0.5 M NaHCO ₃	CO	95	-0.8 V vs. RHE	10	[98]
Ag foil			75		-0.3	
Zn nanosheet	0.5 M NaHCO ₃	CO	86	-1.13 V vs. RHE	6	[99]
Zn foil			9.5		-1	
Sn sheet confined in graphene	0.1 M NaHCO ₃	formate	89	-1.8 V vs. SCE	21.1	[100]
Bulk Sn			44.5		1.6	
Cu nanosheet	0.1 M K ₂ SO ₄	ethylene	83.2	-1.18 V vs. RHE	58.8	[101]
Cu nanoparticles			37.2		36.4	
Sn nanosheet	0.5 M NaHCO ₃	formate	83	-0.9 vs. RHE	14	[102]
Sn foil			25		6	
Cu plates	0.5 M KCl	ethylene	74.9	-0.9 vs. RHE	50	[103]
Cu nanoparticles			52		10	
Zn nanosheet	0.1 M KHCO ₃	CO	90	-1.0 V vs. RHE	100	[104]
Zn nanoparticles			70		50	
Co nanosheet	0.1 M Na ₂ SO ₄	formate	90.1	-0.85 V vs. SCE	10.59	[105]
Bulk Co			25		68.0	
Co ₃ O ₄ nanosheets	0.1 M KHCO ₃	formate	64.3	-0.88 V vs. SCE	0.68	[106]
Bulk Co ₃ O ₄			18.5		0.034	
Bi nanosheet	0.5 M NaHCO ₃	formate	-90	-1.74 V vs. SHE	24	[107]
Bi nanoparticles			-60		6	
ZnO nanosheet	0.1 M KHCO ₃	CO	83	-1.1 V vs. RHE	16.1	[108]
Bi ₂ WO ₆ nanosheet	0.5 M BmimPF ₆ /MeCN	CO	91	-2.4 V vs. Ag/Ag ⁺	43	[109]
N-codoped graphenes nanosheet	0.5 M KHCO ₃	formate	64	-0.80 V vs. RHE	4	[110]
SnS ₂	0.1 M KHCO ₃	formate	93.3	-0.75 V vs. RHE	55	[111]
InN nanosheet	1 M KOH	formate	91	-0.9 V vs. RHE	46	[112]
Mo-Bi bimetallic chalcogenide nanosheet	0.5 M BmimBF ₄ /MeCN	methanol	71.2	-0.7 V vs. SHE	12.1	[85]
FeTPP[Cl]/Cu	1 M KHCO ₃	ethanol	41	-0.82 V vs. SHE	124	[113]

2D: 2-dimensional; FE: Faradaic efficiency.

electro-reduction compared with their nanoparticles. For instance, Lee *et al.* prepared Ag nanosheets [Figure 6A] using a self-organized method and obtained an FE_{CO} of 95% over the Ag nanosheets at an overpotential of only 0.29 V^[98] [Figure 6B and C]. The current density and surface area of the Ag nanosheets are 37 and 17 times higher than those of polycrystalline Ag, indicating that both the enlarged surface area and high current density promoted by the 2D structure determine the catalytic performance. According to scanning transmission electron microscopy (STEM) images, numerous twin crystals exist between and within individual grains of the Ag nanosheets, and these grain boundaries are considered active sites for CO₂ electro-reduction.

Different crystal planes exhibit different catalytic activities for the conversion of CO₂ to products, and thus regulation of the crystal planes of nanosheet is an effective strategy to obtain high current density and FE for certain products. For example, Zhao *et al.* demonstrated that Pd nanosheets prepared by co-precipitation exhibit excellent catalytic activity in the electro-reduction of CO₂ to CO at the moderate overpotential of 590 mV^[118] [Figure 6D-F]. Pd nanosheets with dominant (111) facet sites are transformed into more active (100) sites after 1 h of electrolysis. The reconstruction of crystal planes not only increases the density of active sites but also reduces the binding energy with CO intermediates, leading to high CO selectivity [Figure 6G].

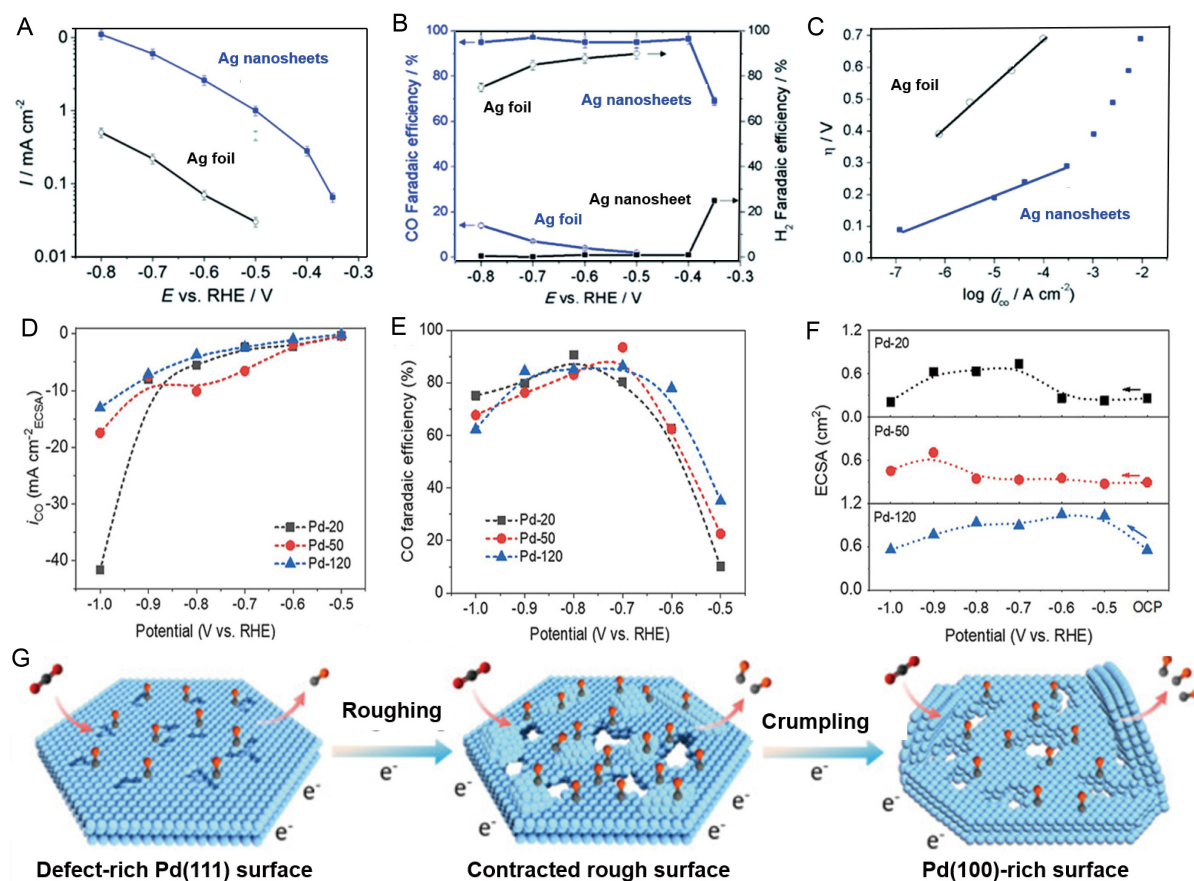


Figure 6. Electrochemical reduction of CO₂ over 2D noble metals. (A) Plot of current density vs. potential over Ag electrodes. (B) FE_{CO} and FE_{H₂} vs. potential over Ag electrodes. (C) Tafel plots^[98]. (D) Plot of current density vs. potential over Pd electrodes. (E) FE_{CO} vs. potential over Pd electrodes. (F) Electrochemical active surface area of different catalysts. (G) Schematic illustration of different Pd materials^[118]. 2D: 2-dimensional.

It is worth mentioning that noble metal nanosheets favor CO over other carbon products of CO₂ electro-reduction because noble metals can strongly adsorb the *COOH intermediate, which is further reduced to CO* on the electrode surface. In addition, CO* is weakly adsorbed on the surface of noble metals, and thus CO easily desorbs from the surface of noble metal nanosheets.

Transition metals

Noble metals are expensive, and thus cost-effective transition metals are increasingly used for CO₂ electro-reduction^[119]. For example, Zn nanosheets prepared by the hydrothermal method perform better than Zn-foil in the electro-reduction of CO₂ and show high selectivity toward CO^[99]. 2D nanostructures exhibit high catalytic activity in CO₂ electro-reduction owing to the high density of edge sites. Xiao *et al.* reported that hexagonal Zn nanoplates prepared by cathodic electrochemical deposition [Figure 7A and B] are suitable for the electrochemical reduction of CO₂ to CO at a wide potential range^[120]. FE_{CO} over Zn nanoplate can reach 94.2%, which is 2.2 times higher than that over Zn foil [Figure 7C]. The high catalytic performance of Zn nanoplates is attributed to the exposed Zn (100) facets and edges, where COOH* can form more easily than at any other facet, indicating that an increased edge-to-corner ratio can enhance the reactivity.

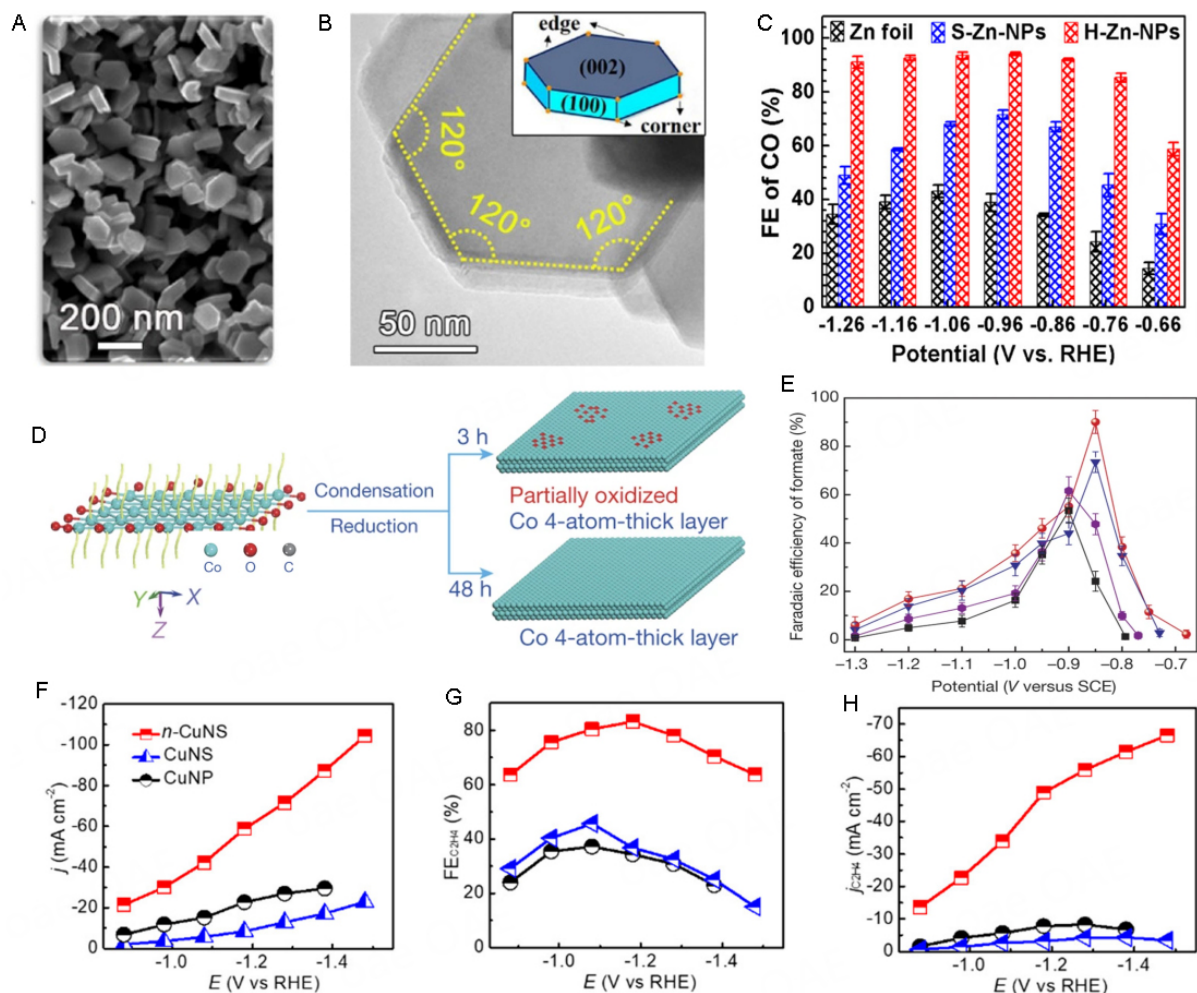


Figure 7. Electrochemical reduction of CO_2 over 2D transition metals. (A) SEM image of hexagonal Zn nanoplates. (B) TEM image of Zn nanoplates. (C) Plot of FE_{CO} vs. potential over different Zn electrodes^[120]. (D) Schematic diagram of the partially oxidized and pure Co 4-atomic-layer. (E) Plot of $\text{FE}_{\text{formate}}$ vs. potential over different Co electrodes^[105]. (F) Plot of current density vs. potential over different Cu electrodes. (G) Plot of $\text{FE}_{\text{C}_2\text{H}_4}$ vs. potential over different Cu electrodes. (H) Plot of $j_{\text{C}_2\text{H}_4}$ vs. potential over different Cu electrodes^[101]. 2D: 2-dimensional; TEM: transmission electron microscopy.

Co is the first transition metal used in CO_2 electro-reduction. Gao *et al.* prepared a 4-atom-thick Co sheet with and without surface Co oxide for CO_2 electro-reduction [Figure 7D], achieving a high $\text{FE}_{\text{formate}}$ of 90.1% at a low overpotential of 0.85 V vs. SCE^[105] [Figure 7E]. Moreover, the catalyst exhibits long-term stability, and FE_{HCOOH} remains at a high level of approximately 90% within 30 h. Volumetric CO_2 adsorption measurements were used to demonstrate that changes in the oxidation state of Co and increases in the surface area synergistically favor CO_2 adsorption, thereby enhancing catalytic performance. Porphyrin Co is one of the most efficient species for CO_2 electro-reduction because of the strong interaction between the metal and ligand. Han *et al.* prepared Co single-site catalysts by assembling Co-porphyrin molecules^[121]. The catalyst can promote the conversion of CO_2 to CO with an FE of 96% at an overpotential of 500 mV. This outstanding catalytic performance is attributed to the increase in the energy of d orbitals originating in the strong repulsive force between the ligand and electrons in the z-direction. Yin *et al.* recently prepared Co nanosheets for the conversion of CO_2 to C_{2+} products^[122]. Co nanoparticles were first prepared by a hydrothermal reaction and then converted to Co nanosheets by exfoliation in formamide. Remarkably, ethanal is the main product of the Co nanosheet electrode with an $\text{FE}_{\text{ethanal}}$ of 60%. Ultraviolet photoelectron

spectroscopy was used to show that Co nanosheets have a wide electronic distribution near the Fermi level, resulting in rapid electron transfer. The electron-rich environment around Co 3d of Co nanosheets is beneficial for CO-CO coupling.

Bi is cheap and environmentally acceptable because of its low toxicity. Bi precursors are used to prepare Bi nanosheets *in situ* by a hydrothermal method^[123], during which O is introduced into the Bi nanosheets. The as-prepared electrode can achieve an $FE_{\text{formic acid}}$ of > 90% with a current density of approximately 200 mA cm⁻² in a flow cell. The catalytic performance remains unchanged when the Bi nanosheets are applied to a long-term test at -0.52 V *vs.* RHE for 10 h. Density functional theory (DFT) calculations suggest that the free energy for *CO₂ → *OCHO is respectively 0.46 eV and 0.17 eV over Bi and Bi-O, indicating that *in situ* construction of Bi nanosheets during electrode fabrication promotes the conversion of CO₂ to formic acid. Yang *et al.* prepared a Bi nanosheet-based catalyst by a solvothermal method, and the as-prepared electrode can achieve an FE_{formate} of nearly 100% over a broad potential range^[124]. Moreover, this electrode exhibits long-term stability at -0.8 V *vs.* RHE for 12 h. DFT calculations demonstrated that Bi(101) and Bi(111) planes can significantly stabilize the COOH* intermediate to promote the formation of formate.

Sn is another transition metal that can be used to convert CO₂ into valuable formate by electrochemical methods. A series of Sn nanosheets have been designed and synthesized for the electro-reduction of CO₂. Wu *et al.* prepared a very sensitive Sn nanosheet with a layer thickness of approximately 9.2 μm by directly spraying Sn catalyst ink onto a gas diffusion layer^[125]. The Sn nanosheet electrode exhibits a high FE_{formate} , owing to the desirable proton concentration, electronic conduction, and gas diffusion of the 2D structure. The thickness of Sn nanosheets also influences the current density, FE, and operating potentials. An ultrathin Sn layer can significantly enhance these reduction-related properties, but an excessively thin layer may increase the oxidation rate of Sn, leading to poor stability. This problem can be resolved by confining metal layers into carbon materials^[126,127]. Lei *et al.* reported a method to prepare Sn quantum sheets confined in graphene^[100]. The confined nanostructure enhances CO₂ adsorption and rate-limiting electron transfer and stabilizes the CO₂^{•-} intermediate. As a result, the graphene confined Sn quantum sheet displays a current density of 21.1 mA cm⁻² and FE_{formate} of 89% at -1.8 V versus SCE, which is higher than that of the mixture of Sn nanoparticles and graphene. Electrochemical impedance spectroscopy was used to confirm the very low interfacial charge-transfer resistance, suggesting that the existence of 2D graphene can improve the conductivity of the electrocatalyst. Moreover, the electronic state of the complex interface can stabilize reaction intermediates, reducing the free energy barrier for the formation of products.

Among the elements, Cu is the most effective in harvesting various products, such as CO, HCOOH, and C₂₊ products, because Cu has a suitable binding energy between products and the surface of catalysts according to the Sabatier principle^[128]. Thus, exploring Cu-based electrodes for CO₂ electro-reduction has become a vigorous research topic. Recently, numerous efforts have been dedicated to developing 2D Cu materials for the electro-reduction of CO₂ to hydrocarbons and alcohols^[129].

In a pioneering work, Hori *et al.* reported the efficient electro-conversion of CO₂ to hydrocarbons and alcohols over an electrodeposited Cu sheet electrode in aqueous inorganic salt solutions^[130]. KCl, K₂SO₄, KClO₄, and dilute HCO₃⁻ electrolytes favor the formation of ethylene and alcohols, while concentrated HCO₃⁻ and phosphate solutions prefer the generation of methane. Zhang *et al.* demonstrated that nanodeficient Cu nanosheets (n-CuNS) effectively reduce CO₂ into C₂ products^[101]. $FE_{\text{C}_2\text{H}_4}$ over n-CuNS electrode is 83.2%, which is higher than that over Cu nanosheets with a smooth surface (CuNS, 45.7%) and Cu nanoparticles (CuNP, 37.2%). The current density and $FE_{\text{C}_2\text{H}_4}$ over different electrodes at different applied potentials are shown in Figure 7F-H. Interestingly, n-CuNS does not produce CO, while CuNS and

CuNP convert CO₂ into CO in high quantities. Therefore, nano defects in Cu nanosheet significantly improve the current density because CO₂ adsorption and C-C coupling are boosted by the enrichment and confinement of reaction intermediates and OH⁻. Chen *et al.* investigated the effects of grain boundary (GB) density and Cu⁺/Cu⁰ ratio during CO₂ electro-reduction^[131]. As the GB density increases, FE_{C₂H₄} first increases and then decreases, which is related to the content of Cu⁺ in the catalyst during the reaction. Therefore, the GB density can activate CO₂ molecules, and Cu⁺ can promote selectivity toward C₂₊ products.

2D metal nanomaterials have highly anisotropic characteristics, abundant coordination sites, and a special electronic structure. Moreover, 2D metals have a unique structure in the absence of external fields, which leads to special properties that can be exploited for electrocatalysis.

Metal oxide materials

Since the pioneering report on the catalytic behaviors of metal oxide semiconductor powders in the 1970s^[132], the past decades have witnessed great progress in the fundamental study of metal oxide catalysts. Semiconductor metal oxides for CO₂ electro-reduction offer several advantages, including low cost, easy maintenance, and the potential to generate C₂₊ products. At present, many kinds of metal oxides have been used for CO₂ electro-reduction. It is worth pointing out that metal oxides are usually unstable and partially or entirely convert to low-valence metal oxide or zero-valence metallic species under negative potentials. Moreover, the final state and reconstruction of electrodes during electrolysis play important roles in CO₂ conversion^[133,134].

Different ZnO nanosheets have been synthesized and employed as excellent electrodes for CO₂ electro-reduction^[135,136]. A series of strategies, such as hydrothermal method, spray-coating, and electrodeposition, was used by Luo *et al.* to prepare ZnO precursors with different morphologies^[137]. ZnO is reconstructed to a porous sheet-like structure, specifically hexagonal Zn crystals, regardless of the initial morphology and reduced to the metallic state during the electrochemistry process. ZnO nanosheets exhibit an FE_{CO} of 91.6% with a current density of 200 mA cm⁻² at -0.62 V *vs.* RHE in a flow reactor. Overall, the reconstruction provides a high surface area, which enhances the catalytic activity and potentially promotes gas diffusion.

In addition to ZnO nanosheets, a number of other 2D metal oxide nanostructures, such as SnO₂, Co₃O₄, and CuO, have been tested for CO₂ electro-reduction. In particular, porous nanosheets are more advantageous. Han *et al.* synthesized porous SnO₂ nanosheets by a two-step method^[102]. A precursor of SnS₂ nanosheets is first obtained by a hydrothermal method and subsequently annealed to obtain SnO₂ nanosheets with a highly porous architecture. The calcination step increases the surface area and active sites of SnO₂, resulting in a small onset potential, large current density, high FE_{HCOOH}, and high stability. Gao *et al.* prepared Co₃O₄ nanolayers for the selective electro-reduction of CO₂ to formate^[138]. The catalyst exhibits good stability, and the current density negligibly changes within 40 h. The materials have abundant oxygen vacancies, which serve as active sites to stabilize reduction intermediates and reduce the activation energy barrier. Moreover, the valence of Co₃O₄ is retained, although the crystal structure is destroyed after the reaction owing to the existence of oxygen vacancies.

CuO is widely used in electro-reduction of CO₂ to C₂₊ products. CuO is reduced to Cu⁺ and metallic Cu during CO₂ electro-reduction^[139,140]. Liu *et al.* prepared an oxygen-rich ultrathin CuO nanoplate for the electro-reduction of CO₂ to C₂H₄ with an FE_{C₂H₄} of 84.5%, which can be maintained for at least 55 h^[103] [Figure 8A]. At the optimal current density of 75 mA cm⁻² and a full-cell voltage of -3.1 V, the FE_{C₂H₄} is 77.3% and the energy efficiency of C₂H₄ is 28.9% [Figure 8B and C]. Cu/Cu₂O heterogeneous interfaces are formed through the self-evolution of CuO nanoplate arrays during electrocatalysis. The impressive

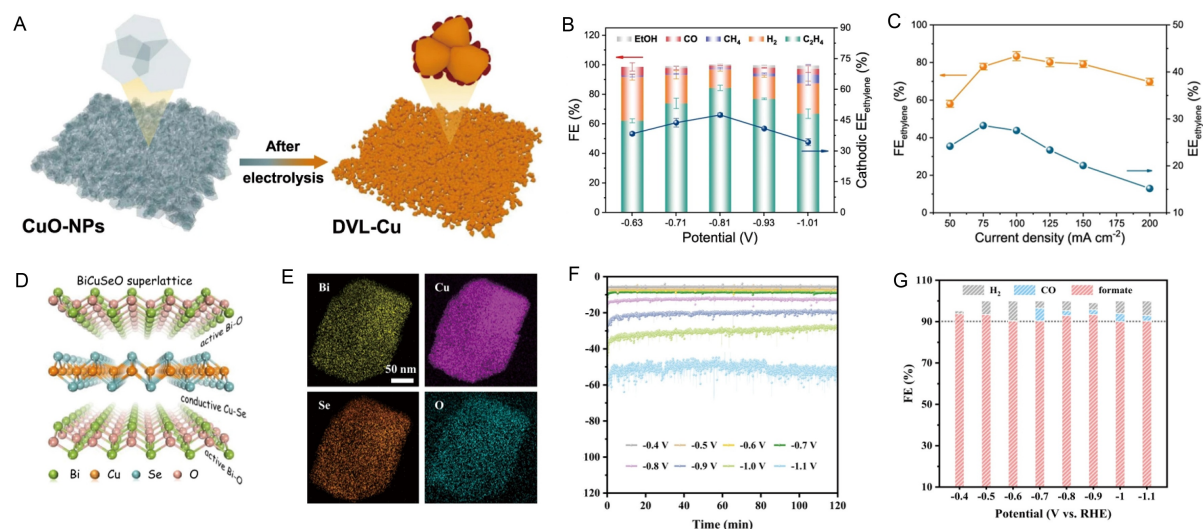


Figure 8. Electrochemical reduction of CO₂ over 2D metal oxides. (A) Schematic illustration of the electrochemical reconstruction of CuO nanosheets. (B) Plot of FE of various products vs. potential over the CuO electrode. (C) Plot of full cell potential and EE_{C₂H₄} vs. current density over the CuO electrode^[103]. (D) Schematic illustration of the BiCuSeO superlattice. (E) EDS mapping images of BiCuSeO. (F) Chronoamperometric curves at different potentials over the BiCuSeO electrode. (G) FE_{formate}, FE_{CO}, and FE_{H₂} vs. potential over the BiCuSeO electrode^[142]. 2D: 2-dimensional; FE: Faradaic efficiency; EDS: energy dispersive spectroscopy.

performance is derived from Cu/Cu₂O interfaces. The enhanced adsorption of the *OCCOH intermediate on the surface of Cu(110)/Cu₂O(110) facilitates the production of C₂H₄. A network comprising Ag and S-Cu₂O/Cu is also formed by the reduction of CuO in Na₂S solution, followed by immersion in AgNO₃ solution^[141]. The as-prepared catalyst exhibits an FE_{CH₃OH} of 67.4% with a current density of approximately 122.7 mA cm⁻² in a typical H-cell at -1.2 V vs. RHE using an ionic liquid (IL)-based electrolyte. Synergistic interaction of multiple atoms in the 2D nanostructure facilitates the practical electro-reduction of CO₂ to methanol. S can control the spatial position of adsorption to accommodate and stabilize the *CHO intermediate, while Ag suppresses the hydrogen evolution reaction (HER) to provide a high FE_{CH₃OH}.

Recently, polymetallic oxides have been developed for CO₂ electro-reduction owing to their structural flexibility. A tangible superlattice model of metal oxide and selenide for CO₂ electro-reduction was demonstrated by Duan *et al.*^[142]. The as-prepared BiCuSeO (layer stacked superlattices) [Figure 8D and E] shows an FE_{formate} of > 90% at a low overpotential [Figure 8F]. The outstanding catalytic activity is attributed to the active 2D Bi₂O₂²⁺ sublayer. It is worth pointing out that the layer-stacked superlattices can inhibit the reduction of metal oxide and HER, resulting in long-term stability and a high FE_{formate} over electrocatalysts [Figure 8G]. Zhao *et al.* reported that 2D ZnGa₂O₄ nanoplates prepared by an ion-exchange method can reduce CO₂ into CO at the relatively low applied potential of -1.4 V vs. Ag/AgCl, with a high FE_{CO} of 96%, owing to the high specific area of the nanoplates^[143]. During CO₂ electro-reduction, partial Zn²⁺ reduces to Zn⁺, and the Zn²⁺/Zn⁺ redox couple favors the activation of CO₂.

2D transition metal oxides have a large specific surface area, atomic-scale thickness, and abundant dangling bonds, leading to high catalytic performance in CO₂ electro-reduction. In principle, metal oxides are first reduced to the corresponding metals, and the as-reduced metal oxides become the active species for CO₂ electro-reduction. Defects and other active components are introduced into the final electrocatalysts during the reduction of metal oxides.

2D metal dichalcogenides

Transition metal dichalcogenides, such as MoS₂, WS₂, MoSe₂ and WSe₂, are common 2D nanostructures and can be easily prepared by simple exfoliation and CVD methods. These materials have a high surface-to-volume ratio and rich active sites, and thus they have the potential to convert CO₂ into valuable products.

During the past decades, MoS₂ has attracted considerable attention owing to its special 2D structure and property. Asadi *et al.* reported that excess d electrons on Mo-edge atoms and a low work function result in high catalytic performance^[144] [Figure 9A and B]. The catalyst shows a current density of 65 mA cm⁻² at -0.764 V *vs.* RHE, at which FE_{CO} reaches 98%. In contrast to bulk MoS₂, the edges of 2D MoS₂ are exposed to the electrolyte, leading to enhanced catalytic effectiveness. Additionally, by tailoring the edge structure of MoS₂, a low onset potential of 31 mV for CO₂ electro-reduction is achievable. 2D VA-Mo_{1-x}M_xS₂ (M = Nb and Ta) materials were prepared by a CVD method and applied as electrodes for CO₂ electro-reduction in an IL-based electrolyte^[145]. The current density of Nb-doped MoS₂ is 50 times higher than that of pristine MoS₂ because doped Nb can shift the center of the d orbitals of Mo edge atoms, leading to weaker binding of CO. However, excessive Nb doping can increase the work function of MoS₂, which has a negative influence on the catalytic performance. Mao *et al.* demonstrated that modulating the MoS₂ edge structure by V, Zr, and Hf can promote the desorption of CO^[146]. It is worth pointing out that dopants located close to the active Mo sites influence the catalytic activity.

Asadi *et al.* also synthesized a series of 2D transition metal dichalcogenides, including MoS₂, WS₂, MoSe₂ and WSe₂, by a chemical vapor transport method for CO₂ electro-reduction^[147]. Among the as-prepared materials, WSe₂ shows the best catalytic performance, leading to an FE_{CO} of 24% with a current density of 18.95 mA cm⁻² at -0.164 V *vs.* RHE (overpotential of 54 mV) in EmimBF₄/H₂O (1:1) solution. The calculated work functions of the four catalysts decrease in the following sequence: MoS₂ > WS₂ > MoSe₂ > WSe₂, in agreement with experimental results.

In addition to 2D transition metal dichalcogenides, other 2D metal sulfides, such as SnS₂, also promote efficient electrochemical reduction of CO₂. Zheng *et al.* prepared SnS₂ nanosheets by an atomic layer deposition method^[111]. Using over 2D SnS₂, the current density and FE_{formate} at -0.75 V *vs.* RHE are 55 mA cm⁻² and 93%, respectively. The catalyst also shows excellent stability, with FE_{formate} decreasing by less than 2% after 40 h of electrolysis. The excellent catalytic performance is attributed to the presence of sulfur atoms on the catalyst surface, which increase the number of undercoordinated sites. A hybrid nanosheet consisting of SnS₂ and H [Figure 9C-F] was investigated by Zhang *et al.*^[148]. The H-SnS₂ catalyst achieves a high FE_{formate} of 93% at -0.9 V *vs.* RHE in 0.1 M KHCO₃ [Figure 9G-I], making it competitive in activity with pristine 2D metal dichalcogenides. The introduction of H onto the surface of the catalyst optimizes the structure of SnS₂ and increases the electron density in adjacent atoms, resulting in a lower reaction barrier for the formation of the HCOO* intermediate.

Transition metal dichalcogenides present a typical sandwich structure in which the metal atomic layer is sandwiched between two layers of sulfur atoms. Although the van der Waals force between each layer is very weak, strong covalent bonds in the plane ensure the stability of the 2D nanostructure. Therefore, 2D transition metal dichalcogenides exhibit excellent stability for long-term CO₂ electro-reduction.

2D carbon-based materials

Carbon-based materials represent a class of submetallic materials owing to the sp² hybrid state and the existence of metallized electrons on the surface. In the past decade, carbon-based materials have received increasing attention for electrocatalysis owing to their active edges, large surface area, and high charge carrier mobility^[149-151]. The ultrahigh surface area and high electron transport along the carbon base plane

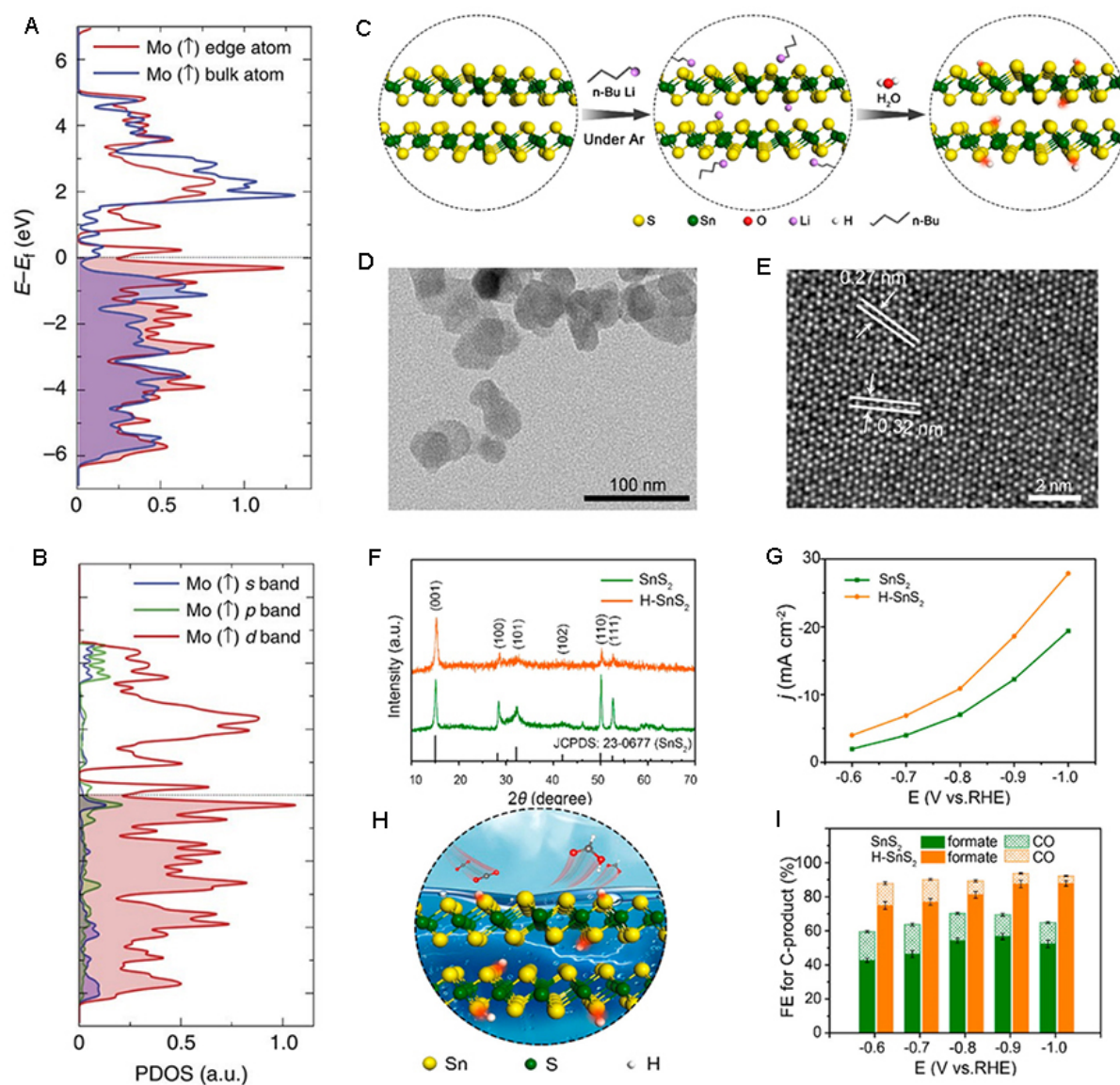


Figure 9. Electrochemical reduction of CO₂ over 2D metal dichalcogenides. (A) PDOS for the spin-up channel of Mo atoms at the edge and within the lattice. (B) PDOS for the spin-up channel of the s, p, and d orbitals of Mo-edge atoms^[144]. (C) Schematic illustration of the synthesis of H-SnS₂ nanosheets. (D) TEM image of H-SnS₂ nanosheets. (E) HRTEM image of H-SnS₂ nanosheets. (F) XRD patterns of H-SnS₂ nanosheets. (G) Plot of current density vs. potential over SnS₂ and H-SnS₂ electrodes. (H) Structural model of H-SnS₂ nanosheets. (I) Plot of FE of products vs. potential over SnS₂ and H-SnS₂ electrodes^[148]. 2D: 2-dimensional; PDOS: projected density of states; TEM: transmission electron microscopy; FE: Faradaic efficiency.

make 2D carbon-based materials suitable for the electrochemical reduction of CO₂.

Graphene is a representative of the carbon family and has been extensively explored in different research fields. Neither pure graphene nor graphene oxide (GO) is active in the electrochemical reduction of CO₂ because the π - π framework cannot effectively activate CO₂^[152]. The electronic structure, physical structure, and morphology of graphene materials can be adjusted by heteroatom doping^[153-155]. N-doped carbon has been widely studied because N is more electronegative than C. Four types of N exist in N-doped graphene: basal plane quaternary N, edge pyrrolic N, pyridinic N, and nitrilic N. Wang *et al.* prepared a nitrogen-doped graphene by high-temperature pyrolysis^[110]. The nitrogen-doped graphene shows high catalytic

activity in the electrochemical conversion of CO₂ to formate, leading to an FE_{formate} of 73%. Recently, many groups have reported that N-doped carbon materials can promote the conversion of CO₂ to C₂ products. For example, Song *et al.* developed a novel method to synthesize nitrogen-doped mesoporous carbon using a copolymer as the template^[156] [Figure 10A]. Pyridinic N sites in this material facilitate the formation of CO*, which is subsequently coupled. Thus, an FE_{ethanol} of 77% at -0.56 V vs. RHE is obtained [Figure 10B-D]. Hao *et al.* also confirmed that pyridinic N promotes efficient CO₂ electro-reduction^[157]. DFT calculations showed that the catalytic activity of different N species in CO formation decreases according to the following sequence: pyridinic N > graphitic N > pyrrolic N [Figure 10E]. Moreover, pyridinic N can also induce C-C coupling^[156], thus boosting the generation of C₂₊ products.

N-doped carbon hybrid nanosheets, normally prepared by wet chemical synthesis, have the advantages of feasible operation, low cost, and large-scale synthesis, and thus they are widely employed as electrodes for the electro-reduction of CO₂. Genovese *et al.* demonstrated that iron (III) oxyhydroxide on nitrogen-doped graphene exhibits an FE_{CH₃COOH} of 61% at -0.5 V vs. Ag/AgCl^[158]. The N-doped graphene not only boosts the activation of CO₂ but also stabilizes Fe(II) species to suppress HER. Lu *et al.* reported that pyridinic N-rich carbon layers encapsulating Ni nanoparticles prepared by a hydrothermal method and pyrolysis exhibit a high FE_{CO} of 95% and long-term stability of 92 h at -1.05 V vs. RHE^[159]. The excellent catalytic performance is attributed to the core-shell structure, which promotes mass transfer and the synergistic effect of N-C and metal oxides, while pyridinic-N increases the CO₂ adsorption capacity and decreases the reaction energy barrier for *COOH formation, the rate-determining step.

Single-atom loaded carbon-based materials are also attractive for CO₂ electro-reduction. Guo *et al.* reported that atomic indium on carbon (In/NC) exhibits a current density of 39.4 mA cm⁻² and FE_{CO} of 97.2% in 0.5 M BmimPF₆/MeCN^[160]. N-coordinated atomic indium catalysts [Figure 10F] can effectively activate CO₂ and hinder the formation of formic acid. In-N coordination is dominant in In/Ac [Figure 10G], indicating that atomic In is stabilized by the surrounding N. Owing to the high double-layer capacitance, large CO₂ adsorption capacity, and low interfacial charge transfer resistance, In/NC achieves a turnover frequency of approximately 40,000 h⁻¹ without appreciable decrease during 24 h of electrolysis [Figure 10H]. DFT results show that the centers of the s and p orbitals of atomic In (In-N) downshift significantly compared with bulk In. A local alkaline environment is produced as the electron density reconfigures because of N coordination. Shi *et al.* reported that Cu single-site in graphdiyne enhances the electro-reduction of CO₂ to methane, with an FE_{CH₄} of 81% and high stability in 1.0 M KOH at -1.2 V vs. RHE^[161]. The acetylenic bond in the catalyst suppresses the formation of multi-carbon products, and the as-constructed Cu-C bond favors the formation of the *OCHO intermediate, resulting in the high FE_{CH₄}.

2D carbon materials, such as graphene, have unique electronic properties, including the ambipolar electric field effect and quantum Hall effect. These unique electronic properties enable carbon materials to exhibit metal-like behaviors, which is beneficial for CO₂ electro-reduction. Moreover, 2D carbon materials are often used as substrates for doping or decoration, broadening their utilizations in CO₂ electro-reduction. Nevertheless, developing highly efficient 2D carbon based materials for CO₂ electro-reduction still has a long way to go.

Other 2D materials

In addition to traditional 2D materials, many other 2D nanostructures are potential candidates to realize highly efficient electro-conversion of CO₂ to valuable products. Recently, a series of novel 2D materials was applied to the electrochemical reduction of CO₂ to various products, and their special structure determines the catalytic performance.

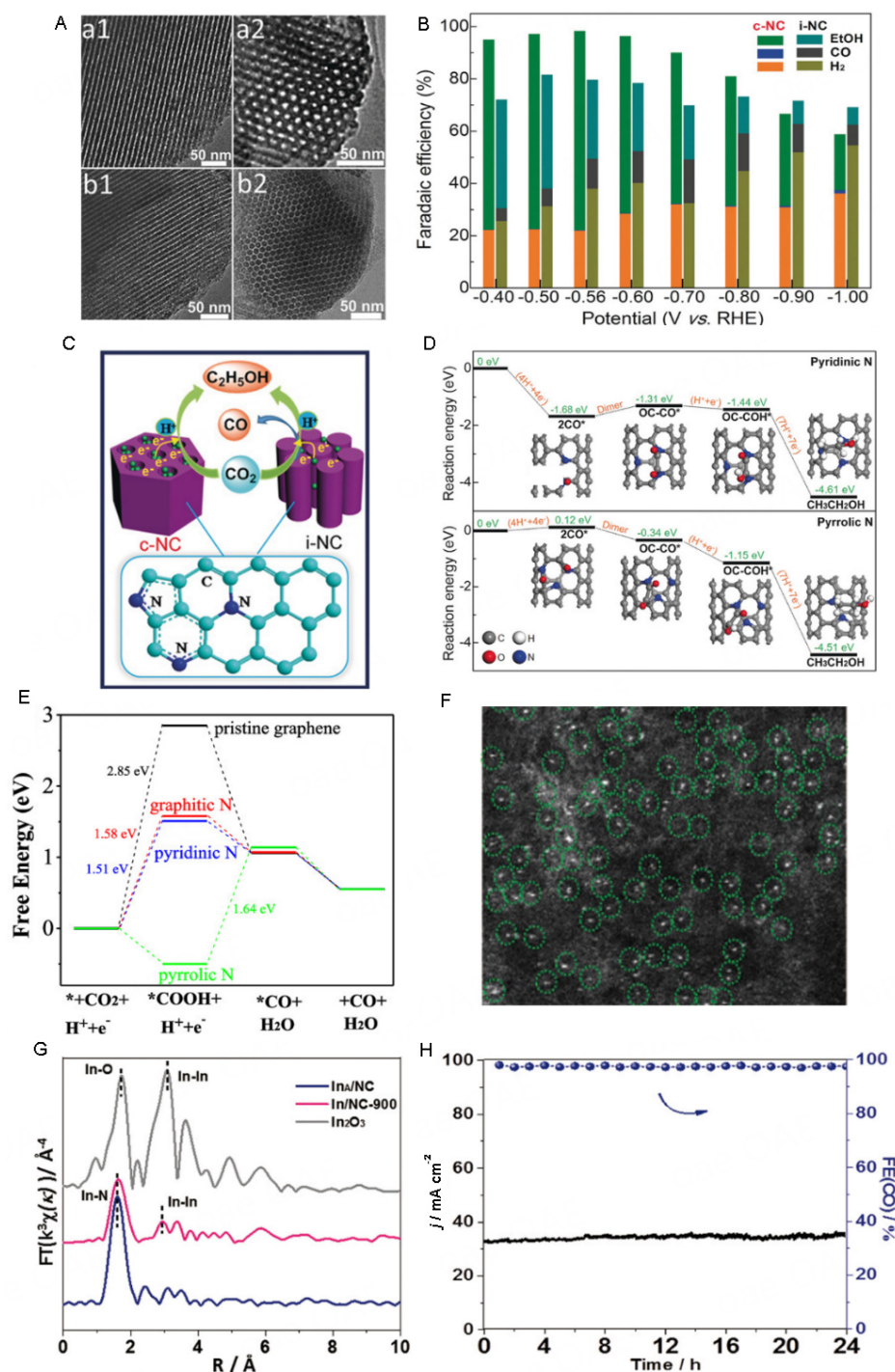


Figure 10. Electrochemical reduction of CO₂ over 2D carbon-based materials. (A) TEM images of nitrogen-doped mesoporous carbons. (B) FEs of various products vs. potential over nitrogen-doped mesoporous carbon electrodes. (C) Schematic illustration of CO₂ electro-reduction over nitrogen-doped mesoporous carbon electrodes. (D) DFT calculations of the electro-reduction of CO₂ to ethanol over different pyrrolic N sites^[156]. (E) Free-energy diagrams of CO₂ electro-reduction over different N species^[157]. (F) Magnified high-angle annular dark-field scanning transmission electron microscopy image of In/NC. (G) Fourier transform of In K-edge extended X-ray absorption fine structure spectra of different In-based catalysts. (H) Long-term stability of CO₂ electro-reduction over In/NC^[160]. 2D: 2-dimensional; TEM: transmission electron microscopy; FE: Faradaic efficiency; DFT: density functional theory.

MOFs have attracted considerable attention in the field of catalysis and energy conversion owing to their

rich active sites, diverse structure, and controllable morphology. Kang *et al.* designed and synthesized a highly efficient MOF catalyst [Cu₂(L)-e/Cu] by *in situ* growth on Cu-foam substrates in IL-based solutions^[162]. MOF particles with assemblies of approximately 50 nm on the surface of the Cu-foam form a thin film [Figure 11A-D]. The MOF thin film contains 15.3% of uncoupled Cu(II) sites, which are considered active sites for the electro-reduction of CO₂ to formic acid. The as-prepared catalyst achieves a high current density of 65.8 mA cm⁻² and FE_{formate} of 90.5% at -1.8 V vs. Ag/Ag⁺ in an IL-based electrolyte [Figure 11E and F]. DFT calculations showed that free Cu(II) centers in defect Cu₂(L) are produced by the rupture of Cu-O bond to promote CO₂ binding.

With their specific layered structure, 2D transition metal carbides and nitrides (MXenes) show high conductivity, high chemical stability, and multiple catalytic sites. Li *et al.* calculated the catalytic activity of single-component MXenes by DFT, and the results showed that Cr₃C₂T_x and Mo₃C₂T_x are the best candidates for the electrochemical reduction of CO₂ to CH₄^[163]. These two materials favor the activation of CO₂ rather than H₂O, resulting in highly efficient CO₂ electro-reduction and HER suppression. Qu *et al.* prepared N-doped Ti₃C₂ MXene nanosheets with abundant titanium vacancies (V_{Ti}) by a facile NH₃-etching pyrolysis approach to achieve an FE_{CO} of 92% and current density of 10 mA cm⁻² at -0.7 V vs. RHE in seawater as the electrolyte^[164]. The coexistence of N and V_{Ti} modulates the electronic structure, leading to a decrease in the reaction energy barriers for *COOH formation.

Molecule-metal catalysts are molecular adsorbates that can accumulate intermediates during CO₂ electro-reduction. Li *et al.* immobilized FeTPP[Cl] onto a Cu substrate to produce a molecular metal catalyst [Figure 11G-I], which was used as an electrode for the electrochemical reduction of CO₂^[113]. FeTPP[Cl] does not reduce into iron nanoparticles or nanoclusters under the operating conditions, and the electrode can achieve an FE_{ethanol} of 41% with a current density of 124 mA cm⁻² at -0.82 V vs. RHE [Figure 11J and K]. *In situ* surface-enhanced Raman spectroscopy and DFT calculations were used to reveal that a local high concentration of CO induced by the electrode promotes C-C coupling to ethanol. Han *et al.* deposited N-substituted pyridinium additives as a film on a Cu electrode for the electro-reduction of CO₂ into C₂₊ products and, furthermore, demonstrated that the film promotes C-C coupling and impedes HER^[165].

Substrates functionalized by molecular monolayers are considered a type of 2D electrodes, which have been extensively studied for CO₂ electro-reduction^[166-169]. For instance, Fang *et al.* reported that a Au electrode modified with 4-pyridylethanemercaptan(4-PEM) exhibits high CO₂ selectivity toward formate compared with pristine Au electrode^[170]. The high surface concentration of H⁺ impedes the first electron transfer to CO₂⁻. Moreover, the organometallic complex was also modified as a gas diffusion layer to fabricate a 2D electrode, which was employed as a cathode in a flow cell microreactor for CO₂ electro-reduction. The electrode exhibits an FE_{HCOOH} of 76% and FE_{CO} of 10%^[171].

Covalent organic frameworks (COFs), composed of organic monomers and hybrid atoms, are new porous organic materials with high crystallinity. Covalent bonds are formed through reversible chemical reactions. COFs have gradually been applied to CO₂ electrocatalysis owing to their designable structure, low density, adjustable pore structure, and easily modified structure. Bando *et al.* synthesized Mn^I tricarbonyl-based 2D COFs for CO₂ electro-reduction^[172]. The as-prepared 2D COFs exhibit a low onset potential of 190 mV, at which a current density of 12 mA cm⁻² and FE_{CO} of 72% are achieved, and the catalyst remains active even after 16 h. Zhu *et al.* developed metalloporphyrin-tetrathiafulvalene-based COFs (M-TTCOFs), which have impressive catalytic performance, achieving an FE_{CO} of > 90% and high cycling stability (> 40 h)^[173]. Tetrathiafulvalene in the 2D nanostructure serves as an electron donor to construct an efficient pathway to accelerate electron transfer and obtain a low activation energy for CO₂ reduction.

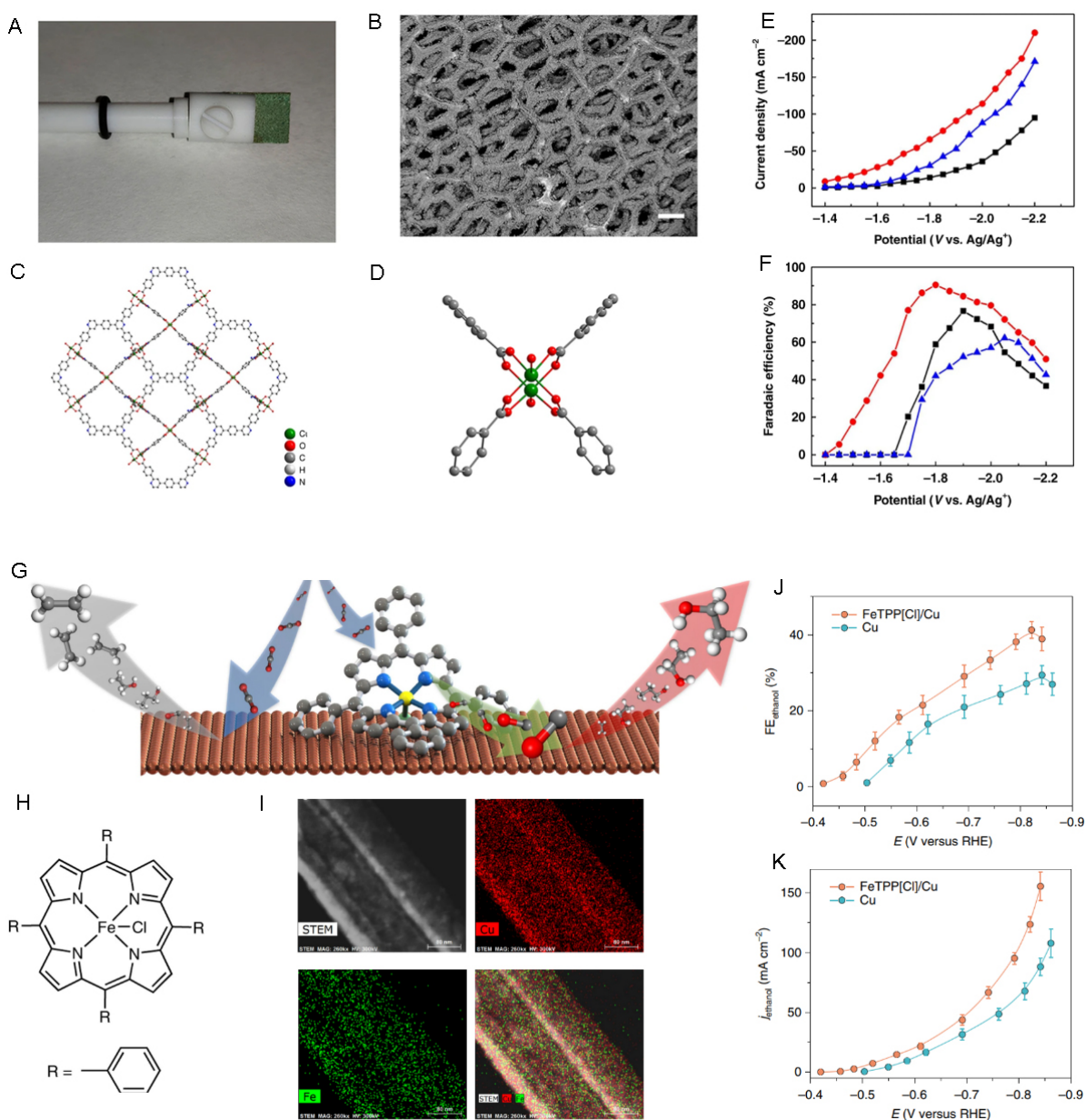


Figure 11. Electrochemical reduction of CO₂ over other 2D materials. (A) Photograph of Cu₂(L)-e/Cu. (B) SEM image of Cu₂(L)-e/Cu. (C and D) Views of the crystal structure of Cu₂(L). (E) Plot of current density vs. potential over Cu₂(L)-e/Cu. (F) Plot of FE_{HCOOH} vs. potential over Cu₂(L)-e/Cu^[62]. (G) Schematic illustration of the heterogenization of molecular complexes on the Cu surface. (H) Molecular structure of FeTPP[Cl]. (I) Elemental mapping of FeTPP[Cl] on Cu. (J) Plot of FE_{ethanol} and (K) j_{ethanol} vs. potential over different electrodes^[13]. 2D: 2-dimensional.

To understand the catalytic nature of 2D materials, the electrochemical properties of the same material with various nanostructures are summarized in Table 1. In general, 2D catalysts exhibit excellent catalytic performance compared with the corresponding bulk catalysts.

SUMMARY AND OUTLOOK

This review summarizes the progress on various 2D materials with a focus on preparation methods and applications to CO₂ electro-reduction. Without any doubt, advances in the synthesis of 2D materials over

the past decade have produced 2D materials that markedly enhance the efficiency of CO₂ electro-reduction.

Methods based on different principles for the preparation of 2D nanostructures have been reviewed. Wet-chemical synthesis and CVD are still the dominant methods for the mass production of 2D materials. It remains urgent to understand how to control the number of layers, flake dimensions, defect levels, and yield of 2D materials. Surface decoration is very important to broaden the application of 2D materials, and it is also an effective way to realize high catalytic performance for CO₂ electro-reduction. Selecting the electrode material is the first step of catalysis. The distribution and production rate of products are determined by the thermodynamic and kinetic energy barriers of reaction pathways. In principle, the electron distribution and the charge density of the catalyst surface affect the kinetic energy barriers. Therefore, selecting electrode materials with appropriate electronic properties can enhance the efficiency of CO₂ electroreduction.

Selectivity is an essential evaluation indicator of the catalytic performance of 2D materials. Although great progress has been made, the reaction pathway determined by the 2D structure is still unclear. In other words, catalytic performance as a function of structural parameters remains unexplored. Strategies such as morphology modification, doping, and surface decoration have been developed to achieve high catalytic performance of 2D materials. Nevertheless, designing *in situ* characterization techniques and developing theoretical calculations to unveil the effect of the structure of 2D materials on CO₂ electro-reduction are highly significant.

Nowadays, high current density can be easily realized by potential increase, structure design, surface functionalization, and cell modification. However, high potentials require high energy consumption, which is inconsistent with the concept of sustainable development. High potentials also influence the long-term stability and promote HER. The surface structure and activity of 2D materials also change under extremely negative potentials. Additionally, most cases of CO₂ electro-reduction over 2D materials are currently being investigated in laboratories owing to the high cost, difficulties in scale-up, and uncontrollable operation. Large-scale synthesis of 2D materials and the preparation of stable and large 2D material-based electrodes are the first important steps into industrialization. We believe that 2D nanostructures will gradually prevail in CO₂ electro-reduction and contribute to carbon neutrality worldwide.

DECLARATIONS

Authors' contributions

Prepared the manuscript: Yin Y

Performed manuscript correcting: Kang X, Han B

Availability of data and materials

Not applicable.

Financial support and sponsorship

This work is supported by National Natural Science Foundation of China (22273108, 22073104) and Beijing Natural Science Foundation (2222043).

Conflict of interest

All authors declared that there are no conflicts of interest.

Ethical approval and consent to participate

Not applicable.

Consent for publication

Not applicable.

Copyright

© The Author(s) 2022.

REFERENCES

1. He M, Sun Y, Han B. Green carbon science: efficient carbon resource processing, utilization, and recycling towards carbon neutrality. *Angew Chem Int Ed Engl* 2022;61:e202112835. DOI PubMed
2. Mehla S, Kandjani AE, Babarao R, et al. Porous crystalline frameworks for thermocatalytic CO₂ reduction: an emerging paradigm. *Energy Environ Sci* 2021;14:320-52. DOI
3. Wu Y, Jiang Z, Lu X, Liang Y, Wang H. Domino electroreduction of CO₂ to methanol on a molecular catalyst. *Nature* 2019;575:639-42. DOI PubMed
4. Yang HB, Hung S, Liu S, et al. Atomically dispersed Ni(I) as the active site for electrochemical CO₂ reduction. *Nat Energy* 2018;3:140-7. DOI
5. Li CW, Ciston J, Kanan MW. Electroreduction of carbon monoxide to liquid fuel on oxide-derived nanocrystalline copper. *Nature* 2014;508:504-7. DOI PubMed
6. Li L, Li X, Sun Y, Xie Y. Rational design of electrocatalytic carbon dioxide reduction for a zero-carbon network. *Chem Soc Rev* 2022;51:1234-52. DOI PubMed
7. Zhang J, An B, Li Z, et al. Neighboring Zn-Zr sites in a metal-organic framework for CO₂ hydrogenation. *J Am Chem Soc* 2021;143:8829-37. DOI PubMed
8. Koshy DM, Nathan SS, Asundi AS, et al. Bridging thermal catalysis and electrocatalysis: catalyzing CO₂ conversion with carbon-based materials. *Angew Chem Int Ed Engl* 2021;60:17472-80. DOI PubMed
9. Sun Q, Wang N, Yu J. Advances in catalytic applications of zeolite-supported metal catalysts. *Adv Mater* 2021;33:e2104442. DOI PubMed
10. Rao H, Schmidt LC, Bonin J, Robert M. Visible-light-driven methane formation from CO₂ with a molecular iron catalyst. *Nature* 2017;548:74-7. DOI PubMed
11. Barman S, Singh A, Rahimi FA, Maji TK. Metal-free catalysis: a redox-active donor-acceptor conjugated microporous polymer for selective visible-light-driven CO₂ reduction to CH₄. *J Am Chem Soc* 2021;143:16284-92. DOI
12. Zhao W, Zhai D, Liu C, et al. Unblocked intramolecular charge transfer for enhanced CO₂ photoreduction enabled by an imidazolium-based ionic conjugated microporous polymer. *Appl Catal B-Environ* 2022;300:120719. DOI
13. Ozden A, Wang Y, Li F, et al. Cascade CO₂ electroreduction enables efficient carbonate-free production of ethylene. *Joule* 2021;5:706-19. DOI
14. Qiu XF, Zhu HL, Huang JR, Liao PQ, Chen XM. Highly selective CO₂ electroreduction to C₂H₄ using a metal-organic framework with dual active sites. *J Am Chem Soc* 2021;143:7242-6. DOI
15. Ma W, Xie S, Liu T, et al. Electrocatalytic reduction of CO₂ to ethylene and ethanol through hydrogen-assisted C-C coupling over fluorine-modified copper. *Nat Catal* 2020;3:478-87. DOI
16. Cheng Y, Hou P, Wang X, Kang P. CO₂ electrolysis system under industrially relevant conditions. *Acc Chem Res* 2022;55:231-40. DOI PubMed
17. Gao D, Wei P, Li H, Lin L, Wang G, Bao X. Designing electrolyzers for electrocatalytic CO₂ reduction. *Acta Phys-Chim Sin* 2021;37:2009021. DOI
18. Li N, Si D, Wu Q, Wu Q, Huang Y, Cao R. Boosting electrocatalytic CO₂ reduction with conjugated bimetallic CO/Zn polyphthalocyanine frameworks. *CCS Chem* 2022. DOI
19. Jia S, Ma X, Sun X, Han B. Electrochemical transformation of CO₂ to value-added chemicals and fuels. *CCS Chem* 2022;4:3213-29. DOI
20. Cheng Y, Hou P, Pan H, Shi H, Kang P. Selective electrocatalytic reduction of carbon dioxide to oxalate by lead tin oxides with low overpotential. *Appl Catal B-Environ* 2020;272:118954. DOI
21. Yang D, Zhu Q, Han B. Electroreduction of CO₂ in ionic liquid-based electrolytes. *Innovation* 2020;1:100016. DOI PubMed PMC
22. Schwarz HA, Dodson RW. Reduction potentials of CO₂⁻ and the alcohol radicals. *J Phys Chem* 1989;93:409-14. DOI
23. Zhao K, Quan X. Carbon-based materials for electrochemical reduction of CO₂ to C₂₊ oxygenates: recent progress and remaining challenges. *ACS Catal* 2021;11:2076-97. DOI
24. Cheng Y, Hou J, Kang P. Integrated capture and electroreduction of flue gas CO₂ to formate using amine functionalized SnO_x nanoparticles. *ACS Energy Lett* 2021;6:3352-8. DOI
25. Chang C, Chen W, Chen Y, et al. Recent progress on two-dimensional materials. *Acta Phys-Chim Sin* 2021;37:2108017. DOI
26. Fu Q, Liu H, Tang X, Wang R, Chen M, Liu Y. Multifunctional two-dimensional polymers for perovskite solar cells with efficiency exceeding 24%. *ACS Energy Lett* 2022;7:1128-36. DOI
27. Song D, Chen X, Lin Z, et al. Usability identification framework and high-throughput screening of two-dimensional materials in

- lithium ion batteries. *ACS Nano* 2021;15:16469-77. DOI PubMed
28. Wang J, Malgras V, Sugahara Y, Yamauchi Y. Electrochemical energy storage performance of 2D nanoarchitected hybrid materials. *Nat Commun* 2021;12:3563. DOI PubMed PMC
29. Liang Q, Zhang Q, Zhao X, Liu M, Wee ATS. Defect engineering of two-dimensional transition-metal dichalcogenides: applications, challenges, and opportunities. *ACS Nano* 2021;15:2165-81. DOI PubMed
30. Shamzhy M, Gil B, Opanasenko M, Roth WJ, Čejka J. MWW and MFI frameworks as model layered zeolites: structures, transformations, properties, and activity. *ACS Catal* 2021;11:2366-96. DOI
31. Xu L, Ma T, Shen Y, et al. Rational manipulation of stacking arrangements in three-dimensional zeolites built from two-dimensional zeolitic nanosheets. *Angew Chem Int Ed Engl* 2020;59:19934-9. DOI PubMed
32. Li G, Shen Y, Zhao S, et al. Construction of rGO-SnO₂ heterojunction for enhanced hydrogen detection. *Appl Surf Sci* 2022;585:152623. DOI
33. Li S, Thiering G, Udvarhelyi P, Ivády V, Gali A. Carbon defect qubit in two-dimensional WS₂. *Nat Commun* 2022;13:1210. DOI PubMed PMC
34. Kovalska E, Antonatos N, Luxa J, Sofer Z. Edge-hydrogenated germanene by electrochemical decalcification-exfoliation of CaGe₂: Germanene-enabled vapor sensor. *ACS Nano* 2021;15:16709-18. DOI PubMed
35. Maiti R, Patil C, Saadi MASR, et al. Strain-engineered high-responsivity MoTe₂ photodetector for silicon photonic integrated circuits. *Nat Photonics* 2020;14:578-84. DOI
36. Liu R, Wang F, Liu L, et al. Band alignment engineering in two-dimensional transition metal dichalcogenide-based heterostructures for photodetectors. *Small Structures* 2021;2:2000136. DOI
37. An C, Nie F, Zhang R, et al. Two-dimensional material-enhanced flexible and self-healable photodetector for large-area photodetection. *Adv Funct Mater* 2021;31:2100136. DOI
38. Wang K, Chen J, Yan X. MXene Ti₃C₂ memristor for neuromorphic behavior and decimal arithmetic operation applications. *Nano Energy* 2021;79:105453. DOI
39. Cao G, Gao C, Wang J, Lan J, Yan X. Memristor based on two-dimensional titania nanosheets for multi-level storage and information processing. *Nano Res* 2022;15:8419-27. DOI
40. Tang B, Veluri H, Li Y, et al. Wafer-scale solution-processed 2D material analog resistive memory array for memory-based computing. *Nat Commun* 2022;13:3037. DOI PubMed PMC
41. Nguyen TN, Salehi M, Le QV, Seifitokaldani A, Dinh CT. Fundamentals of electrochemical CO₂ reduction on single-metal-atom catalysts. *ACS Catal* 2020;10:10068-95. DOI
42. Wang Y, Liu J, Wang Y, Al-Enizi AM, Zheng G. Tuning of CO₂ reduction selectivity on metal electrocatalysts. *Small* 2017;13:1701809. DOI PubMed
43. Shimoni R, Shi Z, Binyamin S, et al. Electrostatic secondary-sphere interactions that facilitate rapid and selective electrocatalytic CO₂ reduction in a fe-porphyrin-based metal-organic framework. *Angew Chem Int Ed Engl* 2022;61:e202206085. DOI PubMed PMC
44. Zhou P, Shen Y, Zhao S, et al. Hydrothermal synthesis of novel ternary hierarchical MoS₂/TiO₂/clinoptilolite nanocomposites with remarkably enhanced visible light response towards xanthates. *Appl Surf Sci* 2021;542:148578. DOI
45. Sun Z, Ma T, Tao H, Fan Q, Han B. Fundamentals and challenges of electrochemical CO₂ reduction using two-dimensional materials. *Chem* 2017;3:560-87. DOI
46. Fang W, Huang L, Zaman S, Wang Z, Han Y, Xia BY. Recent progress on two-dimensional electrocatalysis. *Chem Res Chin Univ* 2020;36:611-21. DOI
47. Li Z, Zhai L, Ge Y, et al. Wet-chemical synthesis of two-dimensional metal nanomaterials for electrocatalysis. *Natl Sci Rev* 2022;9:nwab142. DOI PubMed PMC
48. Ma Y, Shi R, Zhang T. Research progress on triphase interface electrocatalytic carbon dioxide reduction. *Acta Chimica Sinica* 2021;79:369. DOI
49. Pan F, Yang Y. Designing CO₂ reduction electrode materials by morphology and interface engineering. *Energy Environ Sci* 2020;13:2275-309. DOI
50. Gu H, Zhong L, Shi G, et al. Graphdiyne/Graphene heterostructure: a universal 2D scaffold anchoring monodispersed transition-metal phthalocyanines for selective and durable CO₂ electroreduction. *J Am Chem Soc* 2021;143:8679-88. DOI PubMed
51. Chen S, Kang Z, Hu X, et al. Delocalized spin states in 2D atomic layers realizing enhanced electrocatalytic oxygen evolution. *Adv Mater* 2017;29:1701687. DOI PubMed
52. Wang P, Zhao D, Yin L. Two-dimensional matrices confining metal single atoms with enhanced electrochemical reaction kinetics for energy storage applications. *Energy Environ Sci* 2021;14:1794-834. DOI
53. Li X, Wang S, Li L, Zu X, Sun Y, Xie Y. Opportunity of atomically thin two-dimensional catalysts for promoting CO₂ electroreduction. *Acc Chem Res* 2020;53:2964-74. DOI PubMed
54. Rong X, Wang HJ, Lu XL, Si R, Lu TB. Controlled synthesis of a vacancy-defect single-atom catalyst for boosting CO₂ electroreduction. *Angew Chem Int Ed Engl* 2020;59:1961-5. DOI PubMed
55. Pan J, Sun Y, Deng P, et al. Hierarchical and ultrathin copper nanosheets synthesized via galvanic replacement for selective electrocatalytic carbon dioxide conversion to carbon monoxide. *Appl Catal B-environ* 2019;255:117736. DOI
56. Chia X, Pumerá M. Characteristics and performance of two-dimensional materials for electrocatalysis. *Nat Catal* 2018;1:909-21. DOI

57. Li Y, Chen J, Chen S, et al. In situ confined growth of bismuth nanoribbons with active and robust edge sites for boosted CO₂ electroreduction. *ACS Energy Lett* 2022;7:1454-61. DOI
58. Liu W, Qi J, Bai P, Zhang W, Xu L. Utilizing spatial confinement effect of N atoms in micropores of coal-based metal-free material for efficiently electrochemical reduction of carbon dioxide. *Appl Catal B-Environ* 2020;272:118974. DOI
59. Niu ZZ, Gao FY, Zhang XL, et al. Hierarchical copper with inherent hydrophobicity mitigates electrode flooding for high-rate CO₂ Electroreduction to multicarbon products. *J Am Chem Soc* 2021;143:8011-21. DOI PubMed
60. Lv K, Teng C, Shi M, et al. Hydrophobic and electronic properties of the E-MoS₂ nanosheets induced by FAS for the CO₂ electroreduction to syngas with a wide range of CO/H₂ ratios. *Adv Funct Mater* 2018;28:1802339. DOI
61. Zeng L, You C, Hong N, Zhang X, Liang T. Large-scale preparation of 2D metal films by a top-down approach. *Adv Eng Mater* 2020;22:1901359. DOI
62. Xu Y, Sprick RS, Brownbill NJ, et al. Bottom-up wet-chemical synthesis of a two-dimensional porous carbon material with high supercapacitance using a cascade coupling/cyclization route. *J Mater Chem A* 2021;9:3303-8. DOI
63. Watts MC, Picco L, Russell-Pavier FS, et al. Production of phosphorene nanoribbons. *Nature* 2019;568:216-20. DOI PubMed
64. Novoselov KS, Geim AK, Morozov SV, et al. Electric field effect in atomically thin carbon films. *Science* 2004;306:666-9. DOI PubMed
65. Li H, Lu G, Wang Y, et al. Mechanical exfoliation and characterization of single- and few-layer nanosheets of WSe₂, TaS₂, and TaSe₂. *Small* 2013;9:1974-81. DOI PubMed
66. Huang Y, Pan YH, Yang R, et al. Universal mechanical exfoliation of large-area 2D crystals. *Nat Commun* 2020;11:2453. DOI PubMed PMC
67. Coleman JN, Lotya M, O'Neill A, et al. Two-dimensional nanosheets produced by liquid exfoliation of layered materials. *Science* 2011;331:568-71. DOI PubMed
68. Ma R, Sasaki T. Two-dimensional oxide and hydroxide nanosheets: controllable high-quality exfoliation, molecular assembly, and exploration of functionality. *Acc Chem Res* 2015;48:136-43. DOI PubMed
69. Dakhchoune M, Villalobos LF, Semino R, et al. Gas-sieving zeolitic membranes fabricated by condensation of precursor nanosheets. *Nat Mater* 2021;20:362-9. DOI PubMed
70. Obst M, Arnauts G, Cruz AJ, et al. Chemical vapor deposition of ionic liquids for the fabrication of ionogel films and patterns. *Angew Chem Int Ed Engl* 2021;60:25668-73. DOI PubMed
71. Novoselov KS, Mishchenko A, Carvalho A, Castro Neto AH. 2D materials and van der Waals heterostructures. *Science* 2016;353:aac9439. DOI PubMed
72. Kim KS, Zhao Y, Jang H, et al. Large-scale pattern growth of graphene films for stretchable transparent electrodes. *Nature* 2009;457:706-10. DOI PubMed
73. Li X, Cai W, An J, et al. Large-area synthesis of high-quality and uniform graphene films on copper foils. *Science* 2009;324:1312-4. DOI PubMed
74. Browne MP, Novotný F, Manzanares Palenzuela CL, Šturala J, Sofer Z, Pumera M. 2H and 2H/1T-transition metal dichalcogenide films prepared via powderless gas deposition for the hydrogen evolution reaction. *ACS Sustainable Chem Eng* 2019;7:16440-9. DOI
75. Yin C, Gong C, Chu J, et al. Ultrabroadband photodetectors up to 10.6 μm based on 2D Fe₃O₄ nanosheets. *Adv Mater* 2020;32:e2002237. DOI PubMed
76. Zhou J, Lin J, Huang X, et al. A library of atomically thin metal chalcogenides. *Nature* 2018;556:355-9. DOI PubMed
77. Li W, Qiu X, Lv B, et al. Free-standing 2D ironene with magnetic vortex structure at room temperature. *Matter* 2022;5:291-301. DOI
78. Xu T, Li S, Li A, et al. Structural evolution of atomically thin 1T'-MoTe₂ alloyed in chalcogen atmosphere. *Small Struct* 2022;3:2200025. DOI
79. Sun Z, Liao T, Dou Y, et al. Generalized self-assembly of scalable two-dimensional transition metal oxide nanosheets. *Nat Commun* 2014;5:3813. DOI PubMed
80. Peng Y, Tan Q, Huang H, et al. Customization of functional MOFs by a modular design strategy for target applications. *Chem Synth* 2022;2:15. DOI
81. Wang L, Saji SE, Wu L, et al. Emerging synthesis strategies of 2D MOFs for electrical devices and integrated circuits. *Small* 2022;18:e2201642. DOI PubMed
82. Pham HTB, Choi JY, Huang S, et al. Imparting functionality and enhanced surface area to a 2D electrically conductive MOF via macrocyclic linker. *J Am Chem Soc* 2022;144:10615-21. DOI PubMed
83. Zheng Y, Zheng S, Xu Y, Xue H, Liu C, Pang H. Ultrathin two-dimensional cobalt-organic frameworks nanosheets for electrochemical energy storage. *Chem Eng J* 2019;373:1319-28. DOI
84. Sun X, Lu L, Zhu Q, et al. MoP nanoparticles supported on indium-doped porous carbon: outstanding catalysts for highly efficient CO₂ electroreduction. *Angew Chem Int Ed Engl* 2018;57:2427-31. DOI PubMed
85. Sun X, Zhu Q, Kang X, et al. Molybdenum-bismuth bimetallic chalcogenide nanosheets for highly efficient electrocatalytic reduction of carbon dioxide to methanol. *Angew Chem Int Ed Engl* 2016;55:6771-5. DOI PubMed
86. Lu L, Guo W, Chen C, et al. Synthesis of Sn₄P₃/reduced graphene oxide nanocomposites as highly efficient electrocatalysts for CO₂ reduction. *Green Chem* 2020;22:6804-8. DOI
87. Rabiee H, Ge L, Zhang X, et al. Shape-tuned electrodeposition of bismuth-based nanosheets on flow-through hollow fiber gas

- diffusion electrode for high-efficiency CO₂ reduction to formate. *Appl Catal B-environ* 2021;286:119945. DOI
88. Abdelazim NM, Noori YJ, Thomas S, et al. Lateral growth of MoS₂ 2D material semiconductors over an insulator via electrodeposition. *Adv Electron Mater* 2021;7:2100419. DOI
 89. Feng C, Wang F, Liu Z, et al. A self-healing catalyst for electrocatalytic and photoelectrochemical oxygen evolution in highly alkaline conditions. *Nat Commun* 2021;12:5980. DOI PubMed PMC
 90. Shen L, Zhang Q, Luo J, et al. Heteroatoms adjusting amorphous FeMn-based nanosheets via a facile electrodeposition method for full water splitting. *ACS Sustainable Chem Eng* 2021;9:5963-71. DOI
 91. Tan SF, Reidy K, Lee S, et al. Multilayer graphene - a promising electrode material in liquid cell electrochemistry. *Adv Funct Materials* 2021;31:2104628. DOI
 92. Lukatskaya MR, Mashtalir O, Ren CE, et al. Cation intercalation and high volumetric capacitance of two-dimensional titanium carbide. *Science* 2013;341:1502-5. DOI PubMed
 93. Lukatskaya MR, Halim J, Dyatkin B, et al. Room-temperature carbide-derived carbon synthesis by electrochemical etching of MAX phases. *Angew Chem Int Ed Engl* 2014;53:4877-80. DOI PubMed
 94. Ghidui M, Lukatskaya MR, Zhao MQ, Gogotsi Y, Barsoum MW. Conductive two-dimensional titanium carbide "clay" with high volumetric capacitance. *Nature* 2014;516:78-81. DOI PubMed
 95. Liu L, Yang X, Xie Y, et al. A universal lab-on-salt-particle approach to 2D single-layer ordered mesoporous materials. *Adv Mater* 2020;32:e1906653. DOI PubMed
 96. Zhang F, Zhang J, Zhang B, et al. CO₂ controls the oriented growth of metal-organic framework with highly accessible active sites. *Nat Commun* 2020;11:1431. DOI PubMed PMC
 97. Ko KY, Song JG, Kim Y, et al. Improvement of gas-sensing performance of large-area tungsten disulfide nanosheets by surface functionalization. *ACS Nano* 2016;10:9287-96. DOI PubMed
 98. Lee C, Zhao Y, Wang C, Mitchell DRG, Wallace GG. Rapid formation of self-organised Ag nanosheets with high efficiency and selectivity in CO₂ electroreduction to CO. *Sustain Energy Fuels* 2017;1:1023-7. DOI
 99. Zhang T, Li X, Qiu Y, et al. Multilayered Zn nanosheets as an electrocatalyst for efficient electrochemical reduction of CO₂. *J Catal* 2018;357:154-62. DOI
 100. Lei F, Liu W, Sun Y, et al. Metallic tin quantum sheets confined in graphene toward high-efficiency carbon dioxide electroreduction. *Nat Commun* 2016;7:12697. DOI PubMed PMC
 101. Zhang B, Zhang J, Hua M, et al. Highly electrocatalytic ethylene production from CO₂ on nanodeficient Cu nanosheets. *J Am Chem Soc* 2020;142:13606-13. DOI PubMed
 102. Han N, Wang Y, Deng J, et al. Self-templated synthesis of hierarchical mesoporous SnO₂ nanosheets for selective CO₂ reduction. *J Mater Chem A* 2019;7:1267-72. DOI
 103. Liu W, Zhai P, Li A, et al. Electrochemical CO₂ reduction to ethylene by ultrathin CuO nanoplate arrays. *Nat Commun* 2022;13:1877. DOI PubMed PMC
 104. Liu K, Wang J, Shi M, Yan J, Jiang Q. Simultaneous achieving of high faradaic efficiency and CO Partial current density for CO₂ reduction via robust, noble-metal-free Zn nanosheets with favorable adsorption energy. *Adv Energy Mater* 2019;9:1900276. DOI
 105. Gao S, Lin Y, Jiao X, et al. Partially oxidized atomic cobalt layers for carbon dioxide electroreduction to liquid fuel. *Nature* 2016;529:68-71. DOI PubMed
 106. Gao S, Jiao X, Sun Z, et al. Ultrathin CO₃O₄ layers realizing optimized CO₂ electroreduction to formate. *Angew Chem Int Ed Engl* 2016;55:698-702. DOI PubMed
 107. Han N, Wang Y, Yang H, et al. Ultrathin bismuth nanosheets from in situ topotactic transformation for selective electrocatalytic CO₂ reduction to formate. *Nat Commun* 2018;9:1320. DOI PubMed PMC
 108. Geng Z, Kong X, Chen W, et al. Oxygen vacancies in ZnO nanosheets enhance CO₂ electrochemical reduction to CO. *Angew Chem Int Ed Engl* 2018;57:6054-9. DOI PubMed
 109. Chu M, Chen C, Guo W, et al. Enhancing electroreduction of CO₂ over Bi₂WO₆ nanosheets by oxygen vacancies. *Green Chem* 2019;21:2589-93. DOI
 110. Wang H, Chen Y, Hou X, Ma C, Tan T. Nitrogen-doped graphenes as efficient electrocatalysts for the selective reduction of carbon dioxide to formate in aqueous solution. *Green Chem* 2016;18:3250-6. DOI
 111. Zheng X, De Luna P, García de Arquer FP, et al. Sulfur-modulated tin sites enable highly selective electrochemical reduction of CO₂ to formate. *Joule* 2017;1:794-805. DOI
 112. Zhang A, Liang Y, Li H, et al. In-situ surface reconstruction of InN nanosheets for efficient CO₂ electroreduction into formate. *Nano Lett* 2020;20:8229-35. DOI PubMed
 113. Li F, Li YC, Wang Z, et al. Cooperative CO₂-to-ethanol conversion via enriched intermediates at molecule-metal catalyst interfaces. *Nat Catal* 2020;3:75-82. DOI
 114. Yu Y, Lee SJ, Theerthagiri J, et al. Reconciling of experimental and theoretical insights on the electroactive behavior of C/Ni nanoparticles with AuPt alloys for hydrogen evolution efficiency and non-enzymatic sensor. *Chem Eng J* 2022;435:134790. DOI
 115. Yu Y, Lee SJ, Theerthagiri J, Lee Y, Choi MY. Architecting the AuPt alloys for hydrazine oxidation as an anolyte in fuel cell: comparative analysis of hydrazine splitting and water splitting for energy-saving H₂ generation. *Appl Catal B-environ* 2022;316:121603. DOI
 116. Lu Q, Rosen J, Zhou Y, et al. A selective and efficient electrocatalyst for carbon dioxide reduction. *Nat Commun* 2014;5:3242. DOI

[PubMed](#)

117. Mistry H, Reske R, Zeng Z, et al. Exceptional size-dependent activity enhancement in the electroreduction of CO₂ over Au nanoparticles. *J Am Chem Soc* 2014;136:16473-6. [DOI](#) [PubMed](#)
118. Zhao Y, Tan X, Yang W, et al. Surface reconstruction of ultrathin palladium nanosheets during electrocatalytic CO₂ reduction. *Angew Chem Int Ed Engl* 2020;59:21493-8. [DOI](#) [PubMed](#)
119. Wang Z, Li C, Yamauchi Y. Nanostructured nonprecious metal catalysts for electrochemical reduction of carbon dioxide. *Nano Today* 2016;11:373-91. [DOI](#)
120. Xiao J, Gao MR, Liu S, Luo JL. Hexagonal Zn nanoplates enclosed by Zn(100) and Zn(002) facets for highly selective CO₂ electroreduction to CO. *ACS Appl Mater Interfaces* 2020;12:31431-8. [DOI](#)
121. Han J, An P, Liu S, et al. Reordering d orbital energies of single-site catalysts for CO₂ electroreduction. *Angew Chem Int Ed Engl* 2019;58:12711-6. [DOI](#) [PubMed](#)
122. Yin J, Yin Z, Jin J, et al. A new hexagonal cobalt nanosheet catalyst for selective CO₂ conversion to ethanal. *J Am Chem Soc* 2021;143:15335-43. [DOI](#) [PubMed](#)
123. Yang J, Wang X, Qu Y, et al. Bi-based metal-organic framework derived leafy bismuth nanosheets for carbon dioxide electroreduction. *Adv Energy Mater* 2020;10:2001709. [DOI](#)
124. Yang H, Han N, Deng J, et al. Selective CO₂ reduction on 2D mesoporous Bi nanosheets. *Adv Energy Mater* 2018;8:1801536. [DOI](#)
125. Wu J, Sharma PP, Harris BH, Zhou X. Electrochemical reduction of carbon dioxide: IV dependence of the Faradaic efficiency and current density on the microstructure and thickness of tin electrode. *J Power Sources* 2014;258:189-94. [DOI](#)
126. Wu D, Wang X, Fu X, Luo J. Ultrasmall Bi nanoparticles confined in carbon nanosheets as highly active and durable catalysts for CO₂ electroreduction. *Appl Catal B-Environ* 2021;284:119723. [DOI](#)
127. Shifa TA, Vomiero A. Confined catalysis: progress and prospects in energy conversion. *Adv Energy Mater* 2019;9:1902307. [DOI](#)
128. Xiao C, Zhang J. Architectural design for enhanced C₂ product selectivity in electrochemical CO₂ reduction using Cu-based catalysts: a review. *ACS Nano* 2021;15:7975-8000. [DOI](#)
129. Zhang Z, Bian L, Tian H, et al. Tailoring the surface and interface structures of copper-based catalysts for electrochemical reduction of CO₂ to ethylene and ethanol. *Small* 2022;18:e2107450. [DOI](#) [PubMed](#)
130. Hori Y, Murata A, Takahashi R. Formation of hydrocarbons in the electrochemical reduction of carbon dioxide at a copper electrode in aqueous solution. *J Chem Soc, Faraday Trans 1* 1989;85:2309. [DOI](#)
131. Chen C, Sun X, Yan X, et al. A strategy to control the grain boundary density and Cu⁺/Cu⁰ ratio of Cu-based catalysts for efficient electroreduction of CO₂ to C₂ products. *Green Chem* 2020;22:1572-6. [DOI](#)
132. Inoue T, Fujishima A, Konishi S, Honda K. Photoelectrocatalytic reduction of carbon dioxide in aqueous suspensions of semiconductor powders. *Nature* 1979;277:637-8. [DOI](#)
133. Han Z, Han D, Chen Z, et al. Steering surface reconstruction of copper with electrolyte additives for CO₂ electroreduction. *Nat Commun* 2022;13:3158. [DOI](#) [PubMed](#) [PMC](#)
134. Sang J, Wei P, Liu T, et al. A reconstructed Cu₂P₂O₇ catalyst for selective CO₂ electroreduction to multicarbon products. *Angew Chem Int Ed Engl* 2022;61:e202114238. [DOI](#)
135. Xiang Q, Li F, Wang J, et al. Heterostructure of ZnO nanosheets/Zn with a highly enhanced edge surface for efficient CO₂ electrochemical reduction to CO. *ACS Appl Mater Interfaces* 2021;13:10837-44. [DOI](#) [PubMed](#)
136. Sikam P, Takahashi K, Roongcharoen T, et al. Effect of 3d-transition metals doped in ZnO monolayers on the CO₂ electrochemical reduction to valuable products: first principles study. *Appl Surf Sci* 2021;550:149380. [DOI](#)
137. Luo W, Zhang Q, Zhang J, Muioli E, Zhao K, Züttel A. Electrochemical reconstruction of ZnO for selective reduction of CO₂ to CO. *Appl Catal B-Environ* 2020;273:119060. [DOI](#)
138. Gao S, Sun Z, Liu W, et al. Atomic layer confined vacancies for atomic-level insights into carbon dioxide electroreduction. *Nat Commun* 2017;8:14503. [DOI](#) [PubMed](#) [PMC](#)
139. Cheng D, Zhao ZJ, Zhang G, et al. The nature of active sites for carbon dioxide electroreduction over oxide-derived copper catalysts. *Nat Commun* 2021;12:395. [DOI](#) [PubMed](#) [PMC](#)
140. Yuan X, Chen S, Cheng D, et al. Controllable Cu⁰-Cu⁺ sites for electrocatalytic reduction of carbon dioxide. *Angew Chem Int Ed Engl* 2021;60:15344-7. [DOI](#)
141. Li P, Bi J, Liu J, et al. In situ dual doping for constructing efficient CO₂-to-methanol electrocatalysts. *Nat Commun* 2022;13:1965. [DOI](#)
142. Duan J, Liu T, Zhao Y, et al. Active and conductive layer stacked superlattices for highly selective CO₂ electroreduction. *Nat Commun* 2022;13:2039. [DOI](#) [PubMed](#) [PMC](#)
143. Zhao M, Gu Y, Chen P, et al. Highly selective electrochemical CO₂ reduction to CO using a redox-active couple on low-crystallinity mesoporous ZnGa₂O₄ catalyst. *J Mater Chem A* 2019;7:9316-23. [DOI](#)
144. Asadi M, Kumar B, Behranginia A, et al. Robust carbon dioxide reduction on molybdenum disulfide edges. *Nat Commun* 2014;5:4470. [DOI](#) [PubMed](#)
145. Abbasi P, Asadi M, Liu C, et al. Tailoring the edge structure of molybdenum disulfide toward electrocatalytic reduction of carbon dioxide. *ACS Nano* 2017;11:453-60. [DOI](#) [PubMed](#)
146. Mao X, Wang L, Xu Y, Li Y. Modulating the MoS₂ edge structures by doping transition metals for electrocatalytic CO₂ reduction. *J Phys Chem C* 2020;124:10523-9. [DOI](#)

147. Asadi M, Kim K, Liu C, et al. Nanostructured transition metal dichalcogenide electrocatalysts for CO₂ reduction in ionic liquid. *Science* 2016;353:467-70. DOI PubMed
148. Zhang A, Liang Y, Li H, et al. Electronic tuning of SnS₂ nanosheets by hydrogen incorporation for efficient CO₂ electroreduction. *Nano Lett* 2021;21:7789-95. DOI
149. Ma X, Du J, Sun H, et al. Boron, nitrogen co-doped carbon with abundant mesopores for efficient CO₂ electroreduction. *Appl Catal B-Environ* 2021;298:120543. DOI
150. Tuci G, Rossin A, Zhang X, Pham-huu C, Giambastiani G. Exohedrally functionalized carbon-based networks as catalysts for electrochemical syntheses. *Curr Opin Green Sustain Chem* 2022;33:100579. DOI
151. Zhang X, Xue D, Jiang S, et al. Rational confinement engineering of MOF-derived carbon-based electrocatalysts toward CO₂ reduction and O₂ reduction reactions. *InfoMat* 2022;4. DOI
152. Hasani A, Teklagne MA, Do HH, et al. Graphene-based catalysts for electrochemical carbon dioxide reduction. *Carbon Energy* 2020;2:158-75. DOI PubMed PMC
153. Tao H, Gao Y, Talreja N, et al. Two-dimensional nanosheets for electrocatalysis in energy generation and conversion. *J Mater Chem A* 2017;5:7257-84. DOI
154. Wang ZL, Choi J, Xu M, et al. Optimizing electron densities of Ni-N-C complexes by hybrid coordination for efficient electrocatalytic CO₂ reduction. *ChemSusChem* 2020;13:929-37. DOI PubMed
155. Lee SJ, Theerthagiri J, Nithyadharseni P, et al. Heteroatom-doped graphene-based materials for sustainable energy applications: a review. *Renew Sust Energ Rev* 2021;143:110849. DOI
156. Song Y, Chen W, Zhao C, Li S, Wei W, Sun Y. Metal-free nitrogen-doped mesoporous carbon for electroreduction of CO₂ to ethanol. *Angew Chem Int Ed Engl* 2017;56:10840-4. DOI PubMed
157. Hao X, An X, Patil AM, et al. Biomass-derived N-doped carbon for efficient electrocatalytic CO₂ reduction to CO and Zn-CO₂ batteries. *ACS Appl Mater Interfaces* 2021;13:3738-47. DOI
158. Genovese C, Schuster ME, Gibson EK, et al. Operando spectroscopy study of the carbon dioxide electro-reduction by iron species on nitrogen-doped carbon. *Nat Commun* 2018;9:935. DOI PubMed PMC
159. Lu Q, Chen C, Di Q, et al. Dual role of pyridinic-N doping in carbon-coated Ni nanoparticles for highly efficient electrochemical CO₂ reduction to CO over a wide potential range. *ACS Catal* 2022;12:1364-74. DOI
160. Guo W, Tan X, Bi J, et al. Atomic indium catalysts for switching CO₂ electroreduction products from formate to CO. *J Am Chem Soc* 2021;143:6877-85. DOI PubMed
161. Shi G, Xie Y, Du L, et al. Constructing Cu-C bonds in a graphdiyne-regulated Cu single-atom electrocatalyst for CO₂ reduction to CH₄. *Angew Chem Int Ed Engl* 2022;61:e202203569. DOI
162. Kang X, Li L, Sheveleva A, et al. Electro-reduction of carbon dioxide at low over-potential at a metal-organic framework decorated cathode. *Nat Commun* 2020;11:5464. DOI PubMed PMC
163. Li N, Chen X, Ong WJ, et al. Understanding of electrochemical mechanisms for CO₂ capture and conversion into hydrocarbon fuels in transition-metal carbides (MXenes). *ACS Nano* 2017;11:10825-33. DOI
164. Qu D, Peng X, Mi Y, et al. Nitrogen doping and titanium vacancies synergistically promote CO₂ fixation in seawater. *Nanoscale* 2020;12:17191-5. DOI PubMed
165. Han Z, Kortlever R, Chen HY, Peters JC, Agapie T. CO₂ reduction selective for C(≥ 2) products on polycrystalline copper with N-substituted pyridinium additives. *ACS Cent Sci* 2017;3:853-9. DOI
166. Costentin C, Savéant JM. Molecular approach to catalysis of electrochemical reaction in porous films. *Curr Opin Electrochem* 2019;15:58-65. DOI
167. Stuardi FM, Tiozzo A, Rotundo L, Leclaire J, Gobetto R, Nervi C. Efficient electrochemical reduction of CO₂ to formate in methanol solutions by Mn-functionalized electrodes in the presence of amines. *Chem Eur J* 2022;28:e202104377. DOI PubMed PMC
168. McCarthy BD, Beiler AM, Johnson BA, Liseev T, Castner AT, Ott S. Analysis of electrocatalytic metal-organic frameworks. *Coord Chem Rev* 2020;406:213137. DOI PubMed PMC
169. Sun C, Gobetto R, Nervi C. Recent advances in catalytic CO₂ reduction by organometal complexes anchored on modified electrodes. *New J Chem* 2016;40:5656-61. DOI
170. Fang Y, Flake JC. Electrochemical reduction of CO₂ at functionalized Au electrodes. *J Am Chem Soc* 2017;139:3399-405. DOI PubMed
171. Filippi J, Rotundo L, Gobetto R, et al. Turning manganese into gold: efficient electrochemical CO₂ reduction by a fac-Mn(apbpy)(Co)₃Br complex in a gas-liquid interface flow cell. *Chem Eng J* 2021;416:129050. DOI
172. Dubed Bandomo GC, Mondal SS, Franco F, et al. Mechanically constrained catalytic Mn(CO)₃ Br single sites in a two-dimensional covalent organic framework for CO₂ electroreduction in H₂O. *ACS Catal* 2021;11:7210-22. DOI
173. Zhu HJ, Lu M, Wang YR, et al. Efficient electron transmission in covalent organic framework nanosheets for highly active electrocatalytic carbon dioxide reduction. *Nat Commun* 2020;11:497. DOI PubMed PMC